8-2017

Modeling and Analysis of Remote, Off-grid Microgrids

Sreenath Chalil Madathil
Clemson University, sreenathcm@gmail.com

Modeling and Analysis of Remote, Off-grid Microgrids

A Dissertation
Presented to
the Graduate School of
Clemson University

In Partial Fulfillment
of the Requirements for the Degree
Doctor of Philosophy
Industrial Engineering

---

by
Sreenath Chalil Madathil
August 2017

Accepted by:
Dr. Scott J Mason, Committee Chair
Dr. Russell Bent
Dr. Sandra D. Ekşioğlu
Dr. Mary E. Kurz

Abstract

Over the past century the electric power industry has evolved to support the delivery of power over long distances with highly interconnected transmission systems. Despite this evolution, some remote communities are not connected to these systems. These communities rely on small, disconnected distribution systems, i.e., microgrids, to deliver power. Power distribution in most of these remote communities often depend on a type of microgrid called "off-grid microgrids". However, as microgrids often are not held to the same reliability standards as transmission grids, remote communities can be at risk to experience extended blackouts.

Recent trends have also shown an increased use of renewable energy resources in power systems for remote communities. The increased penetration of renewable resources in power generation will require complex decision making when designing a resilient power system. This is mainly due to the stochastic nature of renewable resources that can lead to loss of load or line overload during their operations.

In the first part of this thesis, we develop an optimization model and accompanying solution algorithm for capacity planning and operating microgrids that include N-1 security and other practical modeling features (e.g., AC power flow physics, component efficiencies and thermal limits). We demonstrate the effectiveness of our model and solution approach on two test systems: a modified version of the IEEE 13 node test feeder and a model of a distribution system in a remote Alaskan

community.

Once a tractable algorithm was identified to solve the above problem, we develop a mathematical model that includes topology design of microgrids. The topology design includes building new lines, making redundant lines, and analyzing N-1 contingencies on generators and lines. We develop a rolling horizon algorithm to efficiently analyze the model and demonstrate the strength of our algorithm in the same network.

Finally, we develop a stochastic model that considers generation uncertainties along with N-1 security on generation assets. We develop a chance-constrained model to analyze the efficacy of the problem under consideration and present a case study on an adapted IEEE-13 node network. A successful implementation of this research could help remote communities around the world to enhance their quality of life by providing them with cost-effective, reliable electricity.

Dedication

This thesis is dedicated to three groups of gurus in my life: My guardians, teachers and Gods.

- To my mother, Remani Chalil Madathil, for her perfect upbringing of her child.
- To my father, Haridas Chenicherri Veettil, for his words of wisdom, "there is no substitute for hardwork".
- To my life-coach and my uncle, Narayanan Chalil Madathil (Bavettan), for his prayers and blessings.
- To all my teachers at Clemson University, Federal Institute of Science and Technology (Angamaly), Chinmaya Vidyalaya (Kannur), Sree Vidhyadhiraja Vidya Mandir High School (Thiruvananthapuram), Rani Jai High School (Nirmalagiri), MES Secondary School (Thalassery), Deva Matha Elementary School (Kollam), Eden School (Thalassery) and Sree Narayana Nursery School (Kathiroor).
- To Paradevatha of Chalil Madam Family, God Sree Guruvayoorappan and Goddess Shree Mookambika Devi for their blessings and for enhancing my spiritual inclinations.

Acknowledgments

First of all, I would like to thank Dr. Scott J. Mason, my illustrious advisor, mentor and role model in my professional life. I fall short of words to express my deep sense of gratitude and respect to Dr. Mason for all the support, encouragement, and valuable advice given to me from time to time. I also feel personally indebted to him for the overall achievements I was able to gain under his guidance.

I would also like to thank all the eminent members of my dissertation committee: Dr. Russell Bent, Dr. Sandra D. Ekşioğlu, and Dr. Mary E. Kurz. I am fortunate that I got an opportunity to work with Dr. Bent at Los Alamos National Laboratory (LANL), which helped me to focus my effortss on obtaining a deeper understanding of my doctoral research. I am also extremely thankful to Dr. Ekşioğlu's for the guidance and directions given for completing this project. The support and guidance from Dr. Mary E. Kurz is really valuable and I consider my first assignment as her teaching assistant a blessing as it helped me to experience knowledge sharing firsthand.

I am thankful to Dr. Anand K. Gramopadhye, for all the valuable support and guidance to help complete my graduate course.

I feel really proud to work at LANL under the guidance of great scientists like Dr. Scott Backhaus, Dr. Harsha Nagarajan, Dr. Alessandro Cattaneo, Dr. Emre Yamangil, Dr. Arthur Barnes, and Miles Lubin. I am grateful to them for the valuable support and guidance extended to me to improve my knowledge.

I am also thankful to all the members of faculty and staff at the Department of Industrial Engineering at Clemson University. I would like to make special mentions and thank Martin Clark, Saundra Holland, Jenny Wirtz, Debra Smith, Beverley Robinson, and Jess Lecroy at Clemson for all their support and help. I am also thankful to my energy teammates, especially, Mowen Lu, Shasha Wang, Site Wang, Zahra Azadi, Hadi Karimi, and Antonio Perraudat, and Siddhartha Nambiar.

I would like to thank Kacy Hopwood at LANL for taking care of all documentation and administrative tasks. I also would like to thank my friends and colleagues especially, Drs. Aby Abraham, Githin Alapatt, Myrtede Alfred, Reshmi Koikkara, Jon Lowe, Melissa Paul, Kasin Ransikarbum, and Niratcha Tungtisanon. I am thankful to the support of my pre-grad school friends: Pratheesh Melakam, Mahesh Sreedharan, Heera Pottekkad, Anish Manohar, Seetharaman C N, Senthilkumar Neelamegam, Arvind Kamboj, Nidheesh Divakaraan, Dhanya Gopinathan, Linta Fenu George, and Asha Rani.

This work would not have been possible without the support of my family. I will start with my brother, Dr. Kapil Chalil Madathil, who has provided enormous guidance during various stages of my graduate school. I would like to thank my sister-in-law, Dr. Aparna Ashok, for her everlasting support. I also thank Dr. C K Ashokan and Anupama Ashok for their love. I am also thankful to my cousins Arekh Nambiar, Preethi Dhanvi, Sunil Vijayan, Amita Nambiar, Aneesh P U, Deepthi Rajagopal, Anoop Raghunathan, Shanu Jain, Sreekanth Mavila, and Anusha Raghunath for their love and support in USA. I also would like to share my special gratitude to Dr. Sushama Chalil Madathil, Suja Nambiar and Jyothi Chalil Madathil for their guidance and support. I am also fortunate to have a lot of nieces and nephews who helped me relax during my stressful times. I thank all of them: Siddhartha, Shilpa, Radhika, Prisha, Anika, Aarya, Arjun, and Aadhya. I also have my special love and regards to Sathvika, my Ammalukutty, for bringing extra cheerfulness to my life every day. I thank Ramachandran C V and Sreedevi Mavila for their support and encouragement for my education.

Finally, I would like to thank the most important person in my life, my wife. I am extremely thankful to my beloved wife, Aswathi Nair, for her love, understanding, and full support during my graduate school life. I also would like to thank her parents, Smt. Sudha Madhavan and Sri. V Madhavan Nair, for their prayers and blessings and for their confidence in me while giving away their daughter's hand during our wedding. I am also thankful for all the support from my brothers-in-law Madhusoodhanan Nair and Sreeprasad Nair, and sister-in-law Dr. Chinju Nair.

Thank you for all your encouragement and support!

Contents

List of Tables

List of Figures

Chapter 1

Introduction

There are many remote communities within the United States of America (US) that are either isolated from the national power grid and/or have high costs of electricity generation and distribution due to the high cost of portable fuel storage and transportation [83]. According to the Electricity Monthly Update (EMU) reports from U.S Energy Information Administration (EIA), the states of Alaska and Hawaii have the highest retail cost of electricity [94]. Remote communities often have a network system of distributed energy resources (DER) that consist of small power generating and/or storing systems like diesel generators, small hydro-electric power stations, batteries, and wind turbines that supply power to the communities. Such networks of distributed power systems that are not connected to the national power grid are typically known as "offgrid microgrids".

The generation, transmission, and distribution of electrical energy are vital for the economic development of any country. With the advent of rapid technological advances in power electronics, power systems now involve complex interconnected networks wherein power is generated at specific locations, transmitted over long distances, and then distributed to customers at local neighborhoods. This interconnection of powers systems, also known as grids, provides electricity for houses, businesses, and industries. One of the major drawbacks for these grids is that whenever a part of the grid is affected by either maintenance or an outage, the entire grid is impacted. One such example of the failure of an entire grid is the power blackout in the northeast US in 2003. As utility companies and consumers were not prepared for a blackout on such a large scale, they started to think about alternate sources of energy that are reliable, secure, efficient, and economical. This is when the idea of microgrids came into being.

Microgrids are small networks of energy sources that serve small localities that are composed of generating devices like distributed generators, batteries, and solar panels. These microgrids are often also connected to the main grid and can act as an auxiliary source of energy when needed. As with any new technology option, decision-makers must understand the economic impact of installing a system that provides an alternative source of energy .

In addition to facilitating energy independence in rural communities, microgrids have the potential for improving resilience and reliability in the bulk transmission systems. Resilience is defined as the ability of power system to withstand large-scale, low-frequency events like hurricanes, avalanches, wildfires, earthquakes etc. [31]. Further, the reliability of a power system is defined as its ability to provide uninterrupted power to its consumers even when the network is impacted by sudden perturbation [15]. During large-scale, extreme events such as Superstorm Sandy [56], large parts of the northeastern US's bulk transmission system were de-energized, leaving many communities without power. Microgrids with distributed generation would have allowed these communities to supply power to their customers, where they installed. However, the development and solution of mathematical models that design and operate cost effective and resilient off-grid microgrids pose new challenges in terms of problem complexity.

1.1 Motivation

Many cities in Alaska have experienced power outages due to earthquakes, avalanches, and other similar disasters [29]. These communities could face a lot of danger when the power supply is disrupted. There are many remote communities in the US that are isolated from the national power grid because of geopolitical barriers (*e.g.*, islands like Hawaii and Puerto Rico, and Alaska, which is not a part of the contiguous landmass of the US), who seek to achieve energy independence. These communities often encounter high costs of electricity generation and distribution due to their high costs for energy generation, portable fuel storage and transportation [83].

According to Alaska Electric Light and Power (AELP), approximately 47% of the state's power outages in 2015 were attributed to heavy snow, ice storms, and heavy winds [24]. Extreme climates can also cause trees and other vegetation to fall on power lines in inaccessible areas. Further, many cities in Alaska have had power outages due to earthquakes, avalanches and other similar disasters [29]. These communities clearly face dangers when their power supply is disrupted. One such example would be the inability to operate a portable oxygen generator for patients or people with breathing difficulties in high altitude areas. In fact, people in New Mexico often are forced to connect their portable oxygen generators to their automobile's power outlets to charge the devices during power outages. The implementation of secure, resilient, and economical power generation and transmission networks to these local communities can help improve people's quality of life.

Another motivation for microgrid research is that continuous supply of power is still a dream for many underdeveloped countries. According to Dr. Akinwumi Adesina, the President of the African Development Bank (AfDB), a new plan to provide access to electricity to 205 million people in Africa will enhance the economic development of the whole continent [87]. This new plan calls for the implementation of a large number of both on-grid and off-grid microgrids that use renewable sources of energy. This recommendation for off-grid microgrid usage by the AfDB is a strong endorsement for decentralized power generation techniques. Quality and reliable energy sources will not only help the industrialization of Africa, but also help to provide clean energy to households for cooking and other purposes. With enormous political will and with the help of modern management techniques, the cost-effective and efficient electrification of such underdeveloped countries can be a reality.

1.2 Terminology

Remote communities often have a network of DER that consist of small power generating devices like diesel generators, small hydro-electric power stations, wind turbines and/or power storing devices (*e.g.*, batteries) that store and supply power for their communities. Such networks of distributed power systems that are not connected to the national grid are typically known as **off-grid microgrids** [83]. An illustrative image of an off-grid microgrid is shown in Figure 1.1.

The use of microgrids will not only help customers to reduce their energy costs, but also make them energy independent. According to Kempener *et al.* [49], the implementation of off-grid microgrids can enhance the quality of life for more than 1 billion people who currently have no access to a continuous supply of electricity. The authors also claim that off-grid microgrids are more appropriate for remote communities because of their geographical limitations and the difficulties associated

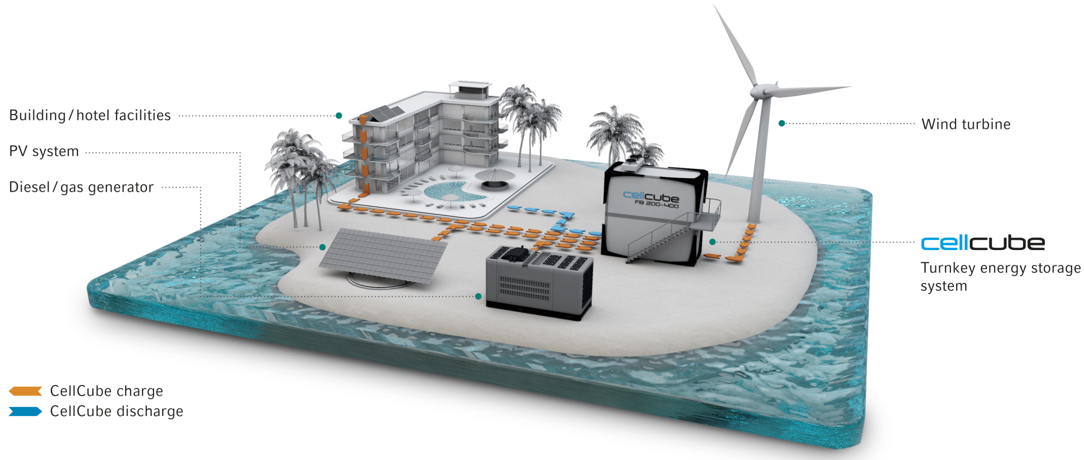

Figure 1.1: An illustration of off-grid microgrid
Source: `http://energy.gildemeister.com/en/utilise/off-gridsolutions`

with extending the national grid to these areas.

Generation assets include various devices or technologies that are used to generate and/or store power. Windmills, photovoltaic (PV) panels, hydro-electric generators, and diesel generators are all examples of generation assets.

Wind generation systems convert wind energy into electrical energy using generators that are connected to windmills. The wind rotates the wheel of a wind turbine which in turn rotates the coils of the generator to produce electricity. The typical parametric data that are required for modelling a wind system includes the wind speed, power output of generators, losses across the system, and the maximum capacity of the generators that can be installed. **Hydro-power plants** use the potential energy of stored water to rotate generators to produce electricity. The input-output characteristics of the generators used in hydro-power plants are the typical data that are required for mathematical modeling. **PV panels** are devices that convert solar energy into electrical energy. They generate direct current (DC) electricity which is normally fed to inverter devices that convert DC to alternating current (AC). Typically, the data that are required to model a PV panel include the power and voltage output from the panel, size of the panel, panel efficiency, and power output degradation over time. All technologies mentioned above are renewable sources of energy.

A **diesel generator** uses diesel as its main fuel to run an engine which is connected to it. The diesel burns inside the engine and converts this energy into mechanical energy which is used to rotate an alternator that generates electric power. Diesel generators typically have minimum up-time, minimum down-time, a ramp-up rate, and a ramp-down rate associated with them. Up-time is the time that the generator should be in the on position and generating power. Down-time is the time that a generator can be in an off position. Finally, ramp-up rate is the rate at which the generator reaches its maximum capacity once it is turned on. These are the typical data and input-output characteristics that are required for modeling generators in mathematical models.

For certain devices like PV panels that generate energy as DC, auxiliary devices are required to convert the energy to AC for power transmission. **Inverters** are devices that convert DC from PV panels or batteries to AC. The losses calculated from the input and output characteristic curves are the only data that is required for modeling inverters. **Batteries** are energy storage devices that are used to generate power when required. The maximum capacity of the battery, rate of charging, and rate of discharging are some of the parameters that are required for modeling these components.

N-1 Secure systems are those power systems that can satisfy all demand in the network even when one of the network's components fail. "N" is the total number of components in the system, like generation units and transmission lines. The "-1" part of N-1 pertains to the failure of one of these components.

1.3 Problem Statement

In this dissertation, we develop a mixed-integer, quadratically constrained, quadratic program (MIQCQP) that minimizes capacity installation cost and operations cost of an off-grid (or disconnected) microgrid. Without connections to local grids, reliability is crucial for such disconnected microgrids. Thus, we also introduce N-1 security constraints to our planning problem. The MIQCQP also models the linearized dist-flow (*LinDistFlow*) [36] ac physics of distribution systems over a full day (in 15 minute intervals) and includes capacity expansion options such as storage and energy sources. We also model the nonlinear efficiency curves associated with these devices using a piecewise linear approximation. We develop a scenario-based decomposition (SBD) algorithm to solve this problem and use both the IEEE 13 node test feeder [50] and a model of a remote community in Alaska to test our proposed approach.

In short, the key contributions of this research are as follows:

- To the best of our knowledge, we develop the first model of distribution system planning that simultaneously includes a nonlinear approximation of ac physics, time-extended operations, capacity expansion, N-1 reliability, and power device efficiencies.
- We include N-1 reliability considerations on generator and line contingencies.
- We develop algorithms that efficiently solve this problem.
- We validate our methods using real system data.
- We model and analyze stochastic power injections in these networks caused by the inclusion of renewable energy sources.

The rest of this dissertation is organized as follows: Chapter 2 introduces the deterministic model to optimally design and operate an offgrid microgrid by considering contingencies for generation assets. Chapter 3 expands the deterministic model to consider contingencies for both generators and lines in the network. Chapter 4 introduces a model for uncertainty in power generation due to wind and solar generation assets. This stochastic model helps determine a strategic plan to design and operate an off-grid microgrid. We conclude our findings and discuss the efficiency of our solution methodologies in Chapter 5, then offer directions for future research.

Chapter 2

Capacity Planning, Operational Planning and N-1 Security

2.1 Introduction

"Energy independence" has been a common topic in most presidential elections in the United States (US) since 1973 [98]. Energy independence can be defined as the state in which national policy decisions on energy generation, transmission, and distribution are made without being influenced by any other external energy producing entities [40]. There are many county governments and local communities in rural areas that need reliable, resilient, and sustainable electrification in addition to reduced dependence on fossil fuel to generate electricity. For these communities, microgrids integrated with local renewable energy sources like solar, wind, and stored water in dams can help to reduce dependence on fossil fuel. The integration of additional generation capabilities could also help these communities to supplement power generation by fossil-fuel based conventional generators [83].

In addition to facilitating energy independence in rural communities, microgrids have the potential for improving resilience and reliability in the bulk transmission systems. During large-scale, extreme events, such as Superstorm Sandy [56], large parts of the bulk transmission system were de-energized, leaving many communities without power. Microgrids with distributed generation would allow these communities to supply power to their customers. Both of these situations present new challenges in reliability in the operation of distribution-scale systems.

In this work, we develop a mixed-integer, quadratically constrained, quadratic programming (MIQCQP) problem that minimizes capacity installation cost and operations cost of an off-grid (or disconnected) microgrid. Without connections to local utility grids, reliability is crucial for such disconnected microgrids. Thus, we introduce N-1 security constraints to our planning problem (Figure 2.1). This flow chart describes the Stages of the problem. At the top are the technology investment variables. The investments are applied at each operating time point (second level of the diagram). The operating decisions are connected via coupling constraints like ramping requirements. Each operating decision is further constrained by contingency requirements in the third stage (the figure only shows contingency constraints for $t = 1$.) The MIQCQP also models the linearized dist-flow (*LinDistFlow*) [36] ac physics of distribution systems over a full day (in 15 minute intervals) and includes capacity expansion options such as storage and energy sources. We also model the nonlinear efficiency curves associated with these devices using a piecewise linear approximation.

We develop a scenario-based decomposition (SBD) algorithm to solve this problem and use both the IEEE 13 node test feeder and a model of a remote community in Alaska to test our approach. In short, the key contributions of this research are:

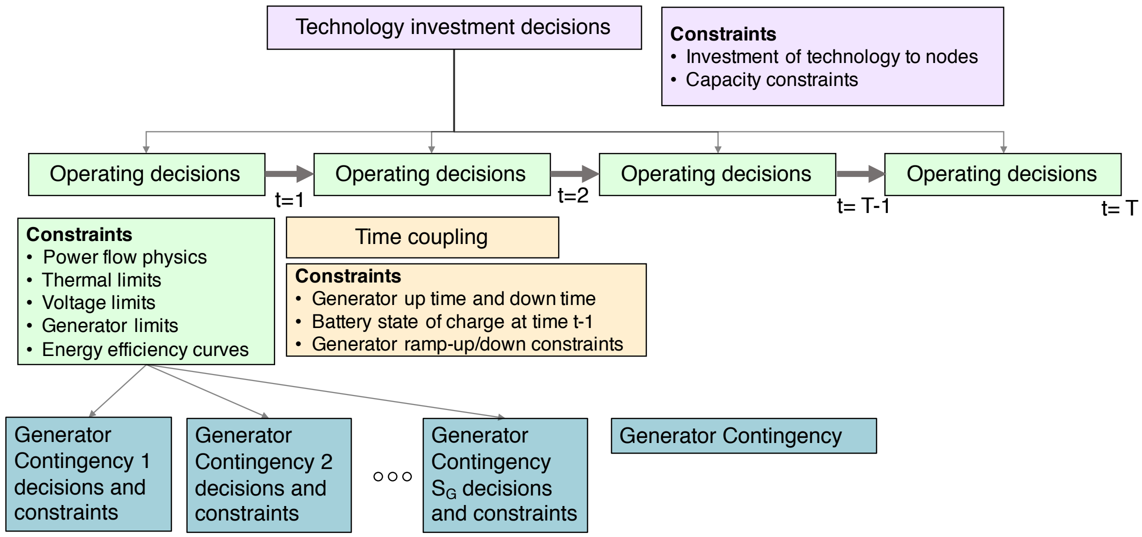

Figure 2.1: Stages of problem development

This flow chart describes the stages of the problem. At the top are the technology investment variables. The investments are applied at each operating time point (second level of the diagram). The operating decisions are connected via coupling constraints like ramping requirements. Each operating decision is further constrained by contingency requirements in the third stage (the figure only shows contingency constraints for $t = 1$)

- To the best of our knowledge, the first model of distribution system planning that simultaneously includes a nonlinear approximation of ac physics, time-extended operations, capacity expansion, N-1 reliability, and power device efficiencies.
- An algorithm that efficiently solves this problem.
- Demonstration on real system data and empirical validation of the results.

2.2 Literature Review

The most similar work to this research is the decision support tool DER-CAM that was developed by Lawrence Berkley National Lab (LBNL). DER-CAM is a decision support tool for decentralized energy systems that is used to plan, install, and operate various distributed energy resources (DER) like distribution generators for buildings and microgrids [17]. DER-CAM is used as a guide to determine technology installations, provide details about operational schedules at each time, and assess the market potential of various technologies for various communities. Baily *et al.* conducted the first study on modeling real-world installations of microgrids by applying the DER-CAM [9]. In many ways, our model is a direct extension of DER-CAM, with a number of key enhancements. In the earliest paper associated with DER-CAM [63], the model focused on designing economical microgrids that satisfy customer demands and power flow physics. The model did not include security constraints, a significant source of computational complexity. In related work [81], authors extended the DER-CAM model and included decision variables associated with DER technology installation, DER capacity, operating status over time, and the cost of electricity. [64] later expanded the model to include an assessment of distribution network reliability. However, they did not include siting of resources or contingencies. Finally, Siddiqui *et al.* [86] discusses various advantages and applications of a localized network of DER.

A common thread in existing work has been a lack of contingency modeling. N-1 contingencies analysis has been studied in the context of transmission systems [95], [70, 21, 88, 72]. This is a rich area of study such as generalizations to unscheduled flows [69]. However, there is only limited work on N-1 (and other types of) security in distribution systems. Hayashi and Matsuki [43] discuss a tabu-search algorithm to determine optimal configuration of a distribution system with N-1 security. The model determines the status of switches, whether it is active or inactive, that connects distribution generators (DG) to the grid.

Concurrent work [66] in DER-CAM strongly motivates the need for N-1

TABLE 2.1: Models used in microgrid design

	Power Flow Physics	Technology Siting	Resource Capacity	Design Horizon	Demand Data	N-1 Security	Efficiencies	Batteries	Comments
[86]	NM	✓	✓	24 hours	hourly	×	×	×	
[68]	CM	✓	✓	24 hours	hourly	×	×	×	Simulation using Homer
[82]	NM	✓	✓	1 year	1 day / month	×	×	✓	
[67]	NM	×	✓	24 hours	hourly	×	×	✓	
[77]	NM	×	✓	24 hours	hourly	×	✓	✓	
[51]	NM	×	×	24 hours	hourly	✓	×	✓	
	LinDistFlow	✓	✓	24 hours	15 minutes	✓	✓	✓	

NM - Network flow Model   CM - Capacity model security with a detailed case study. That paper includes much of the modeling detail included here and uses a linear approximation of the ac physics. Here, we address the scalability issues raised in [66], strengthen the approximation of ac physics with a convex quadratic formulation, and evaluate the quality of solutions obtained with the approximation.

Similar to N-1 security in distribution systems, there is limited work on models that include efficiencies of all components in the system. Bischi *et al.* [16] present a mixed integer linear program (MILP) model for planning the operation of combined cooling heating and power (CCHP) energy systems. They initially modeled the component efficiencies as non-linear constraints and then used a piecewise linearized approximation of the non-linear equations. Bahramirad *et al.* [8] develop a mathematical model to determine optimal sizing of an energy storage system and include constraints on the reliability of the system. They calculated the reliability index as the expected load curtailment in each reduced scenario and constraints are added to limit the loss of load expectation to certain threshold value.

Apart from developing mathematical models for designing and operating microgrids, there are several models that utilize the results of simulations. Hafez and Bhattacharya [42] develop a simulation model for the optimal design, planning, sizing, and operation of a hybrid renewable energy system (HRES). The authors use Homer® to select the capacity of generation and storage resources. More generally, Bahramara *et al.* [7] provide a list of problems that uses Homer software to solve design and operation of HRES. Bie *et al.* [13] use a non-sequential Monte Carlo simulation method to evaluate the reliability of distribution systems by considering multiple contingencies in the network. Table 2.1 lists the most related papers to our work and highlights key differences. Based on Table 2.1, we believe this research is the first to combine N-1 security with the design and operation of off-grid microgrids.

The rest of the chapter is organized as follows: Section II introduces the mathematical formulation for the design and operation of off-grid microgrids with resource siting, power-flow physics, line limits, operational constraints, resource limits and storage efficiency. Section II also discusses the formulation of N-1 security constraints. Section III presents our algorithm for solving the model efficiently. Numerical results on two case studies are discussed in Section IV. Finally, Section V presents conclusions and future directions of research.

2.3 Mathematical Formulation

In this section we introduce the model for operating and planning microgrids for N-1 security. A power system is defined by a graph structure, where nodes correspond to buses and edges correspond to lines and transformers. Each bus may have energy resources that facilitate the production and transfer of power. Energy resources are sized in continuous or discrete capacity increments. For example, solar panels and storage resources, like batteries, are typically modeled as continuous capacity resources, whereas diesel and wind generators are modeled as discrete capacity resources. From an operational standpoint, resources are operated continuously (solar panels, hydro-electric generators, and wind turbines) or can be turned on or off at discrete time intervals (diesel generators). In short, most storage resources are modeled continuously and are classified as continuous operation resources. Generator resources are modeled continuously or discretely depending on their operation requirements. Each bus has a parametrized maximum number of continuous and discrete resources that may be installed. Each discrete resource is assigned to a specific slot (for contingency modeling) at a bus. Slots are used only for discrete resources to identify the number of discrete technology options that can be installed at a bus. We assume that generators that are at nodes with greater than one slot are installed in descending order of their maximum capacity. This assumption drastically increases the computational efficiency by avoiding a combinatorial explosion of possible installations at a node.

2.3.1 Model Parameters and Variables

Sets

N	set of nodes (buses), indexed by i
$\mathcal{E}$	set of existing edges (lines and transformers), indexed by ij
$\mathcal{E}_n$	set of new edges (lines and transformers), indexed by ij
$N^C \subseteq N$	set of nodes with continuous resources, indexed by i
$N^{CB} \subseteq N$	set of nodes with continuous resources with storage capabilities, indexed by i
$N^D \subseteq N$	set of nodes with discrete resources, indexed by i
$N_G(i)$	neighborhood of bus i, indexed by j
$K(i)$	number of slots at bus i, indexed by k_i
T	set of time periods, indexed by t
C	set of continuous resource options, indexed by c
$C^D \subseteq C$	set of continuous resource options with discrete operation, indexed by c
$C^C \subseteq C$	set of continuous resource options with continuous operation, indexed by c

$C^B \subseteq C^C$ set of continuous battery resource options, indexed by c

D set of discrete resource options, indexed by d

$D^D \subseteq D$ set of discrete resource options with discrete operation, index by d

$D^C \subseteq D$ set of discrete resource options with continuous operation, indexed by d

$A = C \cup D$ set of all resource options, indexed by a

S set of scenarios for N-1 security analysis, indexed by s

Parameters

FC_a fixed cost for resource $a \in A$, (\$)

VC_a variable cost for resource $a \in A$, (\$/MW)

$\mathrm{OC}_{a,0}$ fixed operational cost for resource $a \in A$, (\$)

$\mathrm{OC}_{a,1}$ linear operational cost for resource $a \in A$, (\$/MW)

$\mathrm{OC}_{a,2}$ quadratic operational cost for resource $a \in A$, (\$/(MW)^2)

LC_{ij} installation cost for line $ij \in \mathcal{E}_n$, (\$)

UT_d , DT_d minimum up-time and down-time for resource $d \in D$, (time-step)

RU_d , RD_d ramp up and ramp down rate for resource $d \in D$, (MW/time-step)

$\tilde{\mathrm{T}}_{ij}$ apparent power thermal limit on line $ij \in \mathcal{E}$, (MVA)

$\mathrm{Pd}_i^t, \mathrm{Qd}_i^t$ Active and reactive power demand at bus $i \in N$ at time $t \in T$, $(\mathrm{MW}, \mathrm{MVAr})$

$\overline{\mathrm{Pgd}}_d, \overline{\mathrm{Qgd}}_d$ maximum active and reactive power generated by a discrete resource $d \in D$ at time $t \in T$, $(\mathrm{MW}, \mathrm{MVAr})$

$\underline{\mathrm{Pgd}}_d, \underline{\mathrm{Qgd}}_d$ minimum active and reactive power generated by a discrete resource $d \in D$ at time $t \in T$, (MW)

$\overline{\mathrm{Ssc}}_c$ maximum energy storage capacity of the battery, (MVA)

$\underline{\mathrm{V}}_i, \overline{\mathrm{V}}_i$ Squared voltage lower and upper bound at bus $i \in N$, $((kV)^2)$

M_c maximum capacity for continuous resource, (MVA)

P Number of pieces for piecewise linearization

L_a^p Stand-by loss (y intercept) of a resource $a \in A$ for each piecewise function $p \in \{1, .., P\}$, (MW)

η_a^p Marginal efficiency at $\pi_p^a\%$ of maximum rated power for each piece $p \in \{1, .., P\}$, (%)

μ Penalty factor for the power not served

$\mathrm{R}_{ij}, \mathrm{X}_{ij}$ Resistance and reactance of line $ij \in \mathcal{E}$, $(k\Omega)$

Δt time-step, (hr)

C_{num} Maximum number of continuous resources at a bus

Binary decision variables: Discrete technology

$x_{i,d,k}^t$ active/inactive status for generator $d \in D$ at node $i \in N^D$ for slot $k \in K_i$ at time $t \in T$

$y_{i,d,k}^t$ start-up status for generator $d \in D$ at node $i \in N^D$ for slot $k \in K_i$ at time $t \in T$

$w_{i,d,k}^t$ shut-down status for generator $d \in D$ at node $i \in N^D$ for slot $k \in K_i$ at time $t \in T$

$\mathcal{B}\mathrm{gd}_{i,d,k}$ status indicator if discrete resource of type $d \in D$ is built at node $i \in N^D$ for slot $k \in K_i$

Binary decision variables: Continuous resources

$\mathcal{B}\mathrm{gc}_{i,c}$ status indicator if continuous resource of type $c \in C$ is built at node $i \in N^C$

Continuous decision variables: Discrete resources

$\mathrm{Pgd}^t_{i,d,k}$ ac active power generation during time $t \in T$ for slot $k \in K$ at node $i \in N$ using discrete resource $d \in D$, (MW)

$\mathrm{Qgd}^t_{i,d,k}$ ac reactive power generation during time $t \in T$ for slot $k \in K$ at node $i \in N$ using discrete resource $d \in D$, (MVAr)

$\mathrm{Pgd\_in}^t_{i,d,k}$ ac active power generation before losses during time $t \in T$ for slot $k \in K$ at node $i \in N$ using discrete resource $d \in D$, (MW)

Continuous decision variables: Continuous resources

$\mathrm{Pgc}^{\max}_{i,c}, \mathrm{Qgc}^{\max}_{i,c}$ maximum capacity of apparent power generation for continuous resource, $c \in C \setminus C^B$ for node $i \in N$, $(\mathrm{MW}, \mathrm{MVAr})$

$\mathrm{S}^{\max}_{i,c}$ maximum capacity of apparent power generation for continuous battery resource, $c \in C^B$ for node $i \in N$, (MVA)

$\mathrm{Pgc}^t_{i,c}, \mathrm{Qgc}^t_{i,c}$ ac apparent power generation during time $t \in T$ at node $i \in N$ using continuous resource $c \in C$, $(\mathrm{MW}, \mathrm{MVAr})$

$\mathrm{Pgc\_in}^t_{i,c}$ ac active power generation before losses during time $t \in T$ at node $i \in N$ using continuous resource $c \in C$, (MW)

$\mathrm{Ssc}_{i,b}^{t}$	Energy stored (state of charge) in the continuous resource battery $c \in C^B$ at time $t \in T$ at node $i \in N$, (MW-hr)
$\mathrm{Ndk}_{i,k}$	capacity of a slot at a node, $i \in N$ for slot $k \in K$, (MW)

Continuous decision variables: Others

$\mathrm{P}_{ij}^{t}, \mathrm{Q}_{ij}^{t}$	Active and reactive power flow though edge $ij \in \mathcal{E}$ at time $t \in T$, (MW, MVAr)
V_i^t	Squared voltage at node $i \in N$ at time $t \in T$, $((kV)^2)$
$Pns_{i,t}^{s}, Qns_{i,t}^{s}$	apparent power not served at node $i \in N$ at time $t \in T$ due to contingency scenario $s \in S$, (MW, MVAr)

2.3.2 Mathematical Model

The objective function (2.1a) minimizes the total installation and operation cost of energy resources. The installation costs for continuous resources consist of a fixed cost and a sizing (variable) cost while the installation cost for discrete resources consist only of a fixed cost. These costs are equal to zero when a resource is already present. The operating costs of resources are modeled with quadratic functions of the form $CF = aP^2 + bP + c$ [77], where a, b and c are cost coefficients.

$$
\begin{aligned}
&\min \sum_{i \in N^C} \Bigg(\sum_{c \in C} (\mathcal{B}\mathrm{gc}_{i,c})(\mathrm{FC}_c) + \sum_{c \in C \setminus C^B} (\mathrm{Pgc}_{i,c}^{\max})(\mathrm{VC}_c) + \\
&\sum_{c \in C^B} (\mathrm{S}_{i,c}^{\max})(\mathrm{VC}_c) \Bigg) + \sum_{i \in N^D} \sum_{d \in D} \sum_{k \in K_i} (\mathcal{B}\mathrm{gd}_{i,d,k})(\mathrm{FC}_d) + \\
&\sum_{t \in T} \sum_{i \in N^C} \sum_{c \in C \setminus C^B} \big((\mathrm{Pgc\_in}_{i,c}^{t})^2 (\mathrm{OC}_{c,2}) + (\mathrm{Pgc\_in}_{i,c}^{t})(\mathrm{OC}_{c,1}) + (\mathcal{B}\mathrm{gc}_{i,c})(\mathrm{OC}_{c,0}) \big) +
\end{aligned}
$$

$$\sum_{t\in T}\sum_{i\in N^D}\sum_{d\in D}\sum_{k\in K_i}\big((\mathrm{Pgd\_in}^t_{i,d,k})^2(\mathrm{OC}_{d,2}) + (\mathrm{Pgd\_in}^t_{i,d,k})(\mathrm{OC}_{d,1}) + (x^t_{i,d,k})(\mathrm{OC}_{d,0})\big) \tag{2.1a}$$

2.3.3 Power Flows

Nodal flow balance is enforced by constraints (2.2a) and (2.2b). Constraints (2.2c) ensure that line thermal limits are enforced during operations. The linearized version of ac power flow physics is modeled in constraints (2.2d). For computational tractability, we use the single-phase, *LinDistFlow* equations of [36, 12] (the model is convex-quadratic when *LinDistFlow* constraints are added). We show in our empirical results that the approximations are reasonable to use here. Finally, voltage bounds are enforced using constraints (2.2e).

$$\sum_{c\in C}(\mathrm{Pgc}^t_{i,c}) + \sum_{d\in D}\sum_{k\in K_i}(\mathrm{Pgd}^t_{i,d,k}) - (\mathrm{Pd}^t_i) = \sum_{\substack{ij\in\mathcal{E}\\ j\in N_G(i)}}\mathrm{P}^t_{ij} \qquad \forall\, i\in N, t\in T \tag{2.2a}$$

$$\sum_{c\in C}(\mathrm{Qgc}^t_{i,c}) + \sum_{d\in D}\sum_{k\in K_i}(\mathrm{Qgd}^t_{i,d,k}) - (\mathrm{Qd}^t_i) = \sum_{\substack{ij\in\mathcal{E}\\ j\in N_G(i)}}\mathrm{Q}^t_{ij} \qquad \forall\, i\in N, t\in T \tag{2.2b}$$

$$(\mathrm{P}^t_{ij})^2 + (\mathrm{Q}^t_{ij})^2 \le (\tilde{\mathrm{T}}_{ij})^2 \qquad \forall\, ij\in\mathcal{E}, t\in T \tag{2.2c}$$

$$V^t_j = V^t_i - 2(\mathrm{R}_{ij}\mathrm{P}^t_{ij} + \mathrm{X}_{ij}\mathrm{Q}^t_{ij}) \qquad \forall\, ij\in\mathcal{E}, t\in T \tag{2.2d}$$

$$(\underline{\mathrm{V}}_i) \le V^t_i \le (\overline{\mathrm{V}}_i) \qquad \forall\, i\in N, t\in T \tag{2.2e}$$

2.3.4 Resource Limits

Constraints (2.3a) through (2.3c) ensure that the output of continuous resources is limited by the installed capacity. Constraint (2.3d) limits the number of continuous technologies installed per bus. Similarly, constraints (2.3e) and (2.3f) bound the output of discrete resources with continuous operation.

$$\mathrm{Pgc}_{i,c}^{t} \leq \mathrm{Pgc}_{i,c}^{\max} \leq \mathcal{B}\mathrm{gc}_{i,c} M_c \qquad \forall\, i \in N^C, c \in C \setminus C^B, t \in T \tag{2.3a}$$

$$\mathrm{Qgc}_{i,c}^{t} \leq \mathrm{Qgc}_{i,c}^{\max} \leq \mathcal{B}\mathrm{gc}_{i,c} M_c \qquad \forall\, i \in N^C, c \in C, t \in T \tag{2.3b}$$

$$\mathrm{S}_{i,c}^{\max} \leq \mathcal{B}\mathrm{gc}_{i,c} M_c \qquad \forall\, i \in N^{CB}, c \in C^B \tag{2.3c}$$

$$\sum_{c \in C} \mathcal{B}\mathrm{gc}_{i,c} \leq C_{\mathrm{num}} \qquad \forall\, i \in N^C \tag{2.3d}$$

$$\underline{\mathrm{Pgd}}_d \mathcal{B}\mathrm{gd}_{i,d,k} \leq \mathrm{Pgd\_in}_{i,d,k}^{t} \leq \overline{\mathrm{Pgd}}_d \mathcal{B}\mathrm{gd}_{i,d,k} \qquad \forall\, i \in N^D, d \in D^C, k \in K_i, t \in T \tag{2.3e}$$

$$\underline{\mathrm{Qgd}}_d \mathcal{B}\mathrm{gd}_{i,d,k} \leq \mathrm{Qgd}_{i,d,k}^{t} \leq \overline{\mathrm{Qgd}}_d \mathcal{B}\mathrm{gd}_{i,d,k} \qquad \forall\, i \in N^D, d \in D^C, k \in K_i, t \in T \tag{2.3f}$$

2.3.5 Resource Slots

Constraints (2.4a) are assignment constraints that ensure each node's slot contains at most one discrete resource. Constraints (2.4b) and (2.4c) are symmetry-breaking constraints that order slot assignments by resource capacity.

$$\sum_{d \in D} \mathcal{B}\mathrm{gd}_{i,d,k} \leq 1 \qquad \forall\, i \in N^D, k \in K_i \tag{2.4a}$$

$$\mathrm{Ndk}_{i,k} = \sum_{d \in D} \overline{\mathrm{Pgd}}_d \mathcal{B}\mathrm{gd}_{i,d,k} \qquad \forall\, i \in N^D, k \in K_i \tag{2.4b}$$

$$\mathrm{Ndk}_{i,k} \geq \mathrm{Ndk}_{i,k+1} \qquad \forall\, i \in N^D, k \in K_i, k < |K_i| \tag{2.4c}$$

2.3.6 Discrete Operation of Resources

Constraints (2.5a) and (2.5b) link resource output to the active or inactive status of the resource. The resource status is linked to the installation choice through constraints (2.5c). Constraints (2.5d) then ensure that activated discrete resources are active for a minimum time period. Similarly, constraints (2.5e) ensure deactivated resources are inactive for a minimum time period. This is a pessimistic model of generator operations that does not allow the boundary conditions at $t = 0$ or $t = T$ to relax the requirements on UT or DT. Without loss of generality, UT and DT could be adjusted at the boundaries to support more optimistic models of generator operations at the boundaries of the model. Constraints (2.5f) and (2.5g) link the resource indicator variables x, y, and w together. Constraints (2.5h) and (2.5i) enforce resource ramping rates between time periods. Finally, constraints (2.5a) through (2.5i) are applied for all $i \in N^D, d \in D^D, k \in K_i, t \in T$.

$$\underline{\mathrm{Pgd}}_d x^t_{i,d,k} \leq \mathrm{Pgd\_in}^t_{i,d,k} \leq \overline{\mathrm{Pgd}}_d x^t_{i,d,k} \tag{2.5a}$$

$$\underline{\mathrm{Qgd}}_d x^t_{i,d,k} \leq \mathrm{Qgd}^t_{i,d,k} \leq \overline{\mathrm{Qgd}}_d x^t_{i,d,k} \tag{2.5b}$$

$$x^t_{i,d,k} \leq \mathcal{B}\mathrm{gd}_{i,d,k} \tag{2.5c}$$

$$\sum_{j=t}^{t+(\min(\mathrm{UT}_d, T-t))} x^j_{i,d,k} \geq (\mathrm{UT}_d) y^t_{i,d,k} \tag{2.5d}$$

$$\sum_{j=t}^{t+(\min(\mathrm{DT}_d, T-t))} x^j_{i,d,k} \leq (\mathrm{DT}_d)(1 - w^t_{i,d,k}) \tag{2.5e}$$

$$x^t_{i,d,k} = x^{t-1}_{i,d,k} + y^t_{i,d,k} - w^t_{i,d,k} \tag{2.5f}$$

$$y^t_{i,d,k} + w^t_{i,d,k} \leq 1 \tag{2.5g}$$

$$\mathrm{RD}_d \geq \mathrm{Pgd}^{t-1}_{i,d,k} - \mathrm{Pgd}^t_{i,d,k} - \overline{\mathrm{Pgd}}_d w^t_{i,d,k} \tag{2.5h}$$

$$\mathrm{RU}_d \geq \mathrm{Pgd}^t_{i,d,k} - \mathrm{Pgd}^{t-1}_{i,d,k} - \overline{\mathrm{Pgd}}_d y^t_{i,d,k} \tag{2.5i}$$

2.3.7 Storage

Apparent power limits on charging and discharging are stated in constraints (2.6a). Constraints (2.6b) link the state of charge to energy extraction, while constraints (2.6c) bounds storage charging and discharging with maximum charging and discharging capacity. The charging and discharging constraints are modelled using the constraints presented by Iordanis *et al.* [54]. Constraints (2.6a) through (2.6c) are applied to all $i \in N^{CB},\ c \in C^{B},\ t \in T$.

$$(\mathrm{Pgc}_{i,c}^{t})^2 + (\mathrm{Qgc}_{i,c}^{t})^2 \leq (\mathrm{S}_{i,c}^{\max})^2 \tag{2.6a}$$

$$\mathrm{Ssc}_{i,c}^{t} = \mathrm{Ssc}_{i,c}^{t-1} - \mathrm{Pgc\_in}_{i,c}^{t}\Delta t \tag{2.6b}$$

$$0 \leq \mathrm{Ssc}_{i,c}^{t} \leq \overline{Ssc_c} \tag{2.6c}$$

2.3.8 Efficiencies

Fig. 2.2 depicts an example of a piecewise linear convex relaxation of the relationship between power generated in kW and output power in kW. The power curves, efficiencies, and specifications of various resources are found in [18], [53], [26], [1] and [75]. We parametrized these piecewise linear relaxed efficiency curve using these specification sheets, however, these choices are provided as user input. More specifically, the input-output relationship is a set of linear functions defined by

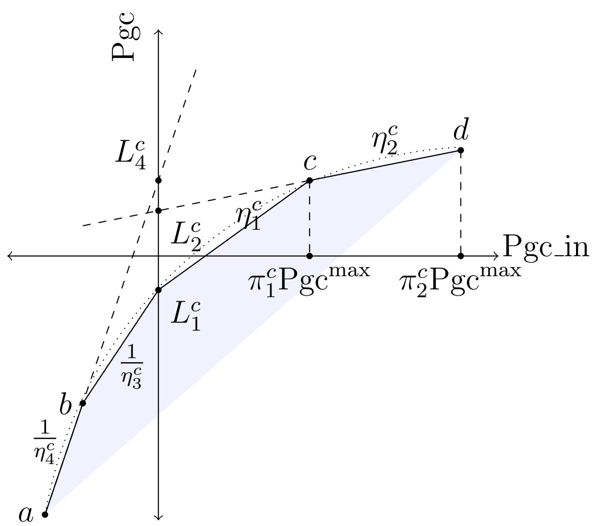

Figure 2.2: An illustrative example of a piecewise linear efficiency curve

constraints (2.7a) through (2.7c) that apply efficiency curves to continuous as well as discrete resources at all nodes $i \in N$, time periods $t \in T$ and slots $k \in K_i$ for each linearization of piecewise function $p \in \{1, .., P\}$. In our models we have used $P = 4$.

$$\mathrm{Pgc}_{i,c}^{t} \leq \eta_c^p \mathrm{Pgc\_in}_{i,c}^{t} + \mathcal{B}\mathrm{gc}_{i,c} L_c^p \qquad \forall\ c \in C \tag{2.7a}$$

$$\mathrm{Pgd}_{i,d,k}^{t} \leq \eta_d^p \mathrm{Pgd\_in}_{i,d,k}^{t} + x_{i,d,k}^{t} L_d^p \qquad \forall\ d \in D^C \tag{2.7b}$$

$$\mathrm{Pgd}_{i,d,k}^{t} \leq \eta_d^p \mathrm{Pgd\_in}_{i,d,k}^{t} + \mathcal{B}\mathrm{gd}_{i,d,k} L_d^p \qquad \forall\ d \in D^D \tag{2.7c}$$

2.3.9 N-1 Security Constraints

In this section, we generalize our model to include security constraints. Without loss of generality, we assume the contingencies are N-1 line and generator contingencies[1]. Once again, without loss of generality, in this study we only include continuous generators and the largest-capacity discrete generators in the security analysis set.

2.3.10 Objective Function

In objective function (2.8a), we add variables that account for the amount of power that is not served during each of the contingencies to the objective function defined in (2.1a), where μ is a penalty variable that penalizes power-not-served (PNS). Decision variables $Pns_{i,t}^{s}$, and $Qns_{i,t}^{s}$ are unrestricted shedding variables that measure the active and reactive power that are not served. Generally, $Pns = 0$ is the goal for all contingencies.

$$\min\ (2.1a)\ + \mu\left(\sum_{i \in N} \sum_{t \in T} \sum_{s \in S} (|Pns_{i,t}^{s}| + |Qns_{i,t}^{s}|) \right) \tag{2.8a}$$

[1]The formulation can include a subset of N-1 contingencies or include sets of N-K contingencies

2.3.11 Power Flows During Contingencies

Contingency variables for power flow variables are indexed by $s \in S$, such as $\mathrm{Pgc}_{i,c}^{t,s}$, $\mathrm{Pgd}_{i,d,k}^{t,s}$, $\mathrm{P}_{ij}^{t,s}$, $\mathrm{Qgc}_{i,c}^{t,s}$, $\mathrm{Qgd}_{i,d,k}^{t,s}$, $\mathrm{Q}_{ij}^{t,s}$, and $\mathrm{V}_i^{t,s}$. For N-1 security analysis, we add new variables to the power flow constraints defined in (2.2a) and (2.2b) of the base model. The power flow equations include PNS for active ($Pns_{i,t}^s$) and reactive power ($Qns_{i,t}^s$) load shedding.

$$Pns_{i,t}^s + \sum_{c \in C}(\mathrm{Pgc}_{i,c}^{t,s}) + \sum_{d \in D}\sum_{k \in K_i}(\mathrm{Pgd}_{i,d,k}^{t,s}) - (\mathrm{Pd}_i^t) = \sum_{\substack{ij \in \mathcal{E} \\ j \in N_G(i)}} \mathrm{P}_{ij}^{t,s} \quad \forall\ i \in N, t \in T, s \in S \tag{2.9a}$$

$$Qns_{i,t}^s + \sum_{c \in C}(\mathrm{Qgc}_{i,c}^{t,s}) + \sum_{d \in D}\sum_{k \in K_i}(\mathrm{Qgd}_{i,d,k}^{t,s}) - (\mathrm{Qd}_i^t) = \sum_{\substack{ij \in \mathcal{E} \\ j \in N_G(i)}} \mathrm{Q}_{ij}^{t,s} \quad \forall\ i \in N, t \in T, s \in S \tag{2.9b}$$

The thermal limit for security analysis is enforced using constraint (2.10a) and *LinDistFlow* is enforced by constraints (2.10b). The voltage limits are constrained by the constraints (2.10c). The constraints (2.10a) through (2.10c) are applied $\forall\ (i,j) \in N, ij \in \mathcal{E}, t \in T, s \in S$.

$$(\mathrm{P}_{ij}^{t,s})^2 + (\mathrm{Q}_{ij}^{t,s})^2 \leq (\tilde{\mathrm{T}}_{ij})^2 \tag{2.10a}$$

$$\mathrm{V}_j^{t,s} = \mathrm{V}_i^{t,s} - 2(\mathrm{R}_{ij}\mathrm{P}_{ij}^{t,s} + \mathrm{X}_{ij}\mathrm{Q}_{ij}^{t,s}) \tag{2.10b}$$

$$\underline{\mathrm{V}_i} \leq \mathrm{V}_i^{t,s} \leq \overline{\mathrm{V}_i} \tag{2.10c}$$

2.3.12 Discrete Resources Contingency

Contingency scenario for the discrete resources is modeled using constraints (2.11a). The indexes in constraints (2.11a) i, d, k, and t represent the contingent scenario $s \in S$ which includes generator d installed at slot $k = 1$ of node i that faults during time t. The discrete resources and ramp factors (Δd_d) are tied to the resources' active/inactive variable $x^t_{i,d,k}$, whereas discrete resources with continuous operation are tied to the installation variable, $\mathcal{B}\mathrm{gd}_{i,d,k}$. Constraints (2.11b) through (2.11e) are applied for all non-contingent discrete resources that belongs to $i \in N, k \in K_i, t \in T$.

$$\mathrm{Pgd}^{t,s}_{i,d,k} = 0, \qquad \mathrm{Qgd}^{t,s}_{i,d,k} = 0 \qquad \forall\ d \in D \tag{2.11a}$$

$$\mathrm{Pgd}^{t}_{i,d,k} - \Delta d_d x^t_{i,d,k} \leq \mathrm{Pgd}^{t,s}_{i,d,k} \leq \mathrm{Pgd}^{t}_{i,d,k} + \Delta d_d x^t_{i,d,k} \qquad \forall\ d \in D^D \tag{2.11b}$$

$$\mathrm{Qgd}^{t}_{i,d,k} - \Delta d_d x^t_{i,d,k} \leq \mathrm{Qgd}^{t,s}_{i,d,k} \leq \mathrm{Qgd}^{t}_{i,d,k} + \Delta d_d x^t_{i,d,k} \qquad \forall\ d \in D^D \tag{2.11c}$$

$$\mathrm{Pgd}^{t}_{i,d,k} - \Delta d_d \mathcal{B}\mathrm{gd}_{i,d,k} \leq \mathrm{Pgd}^{t,s}_{i,d,k} \leq \mathrm{Pgd}^{t}_{i,d,k} + \Delta d_d \mathcal{B}\mathrm{gd}_{i,d,k} \qquad \forall\ d \in D^C \tag{2.11d}$$

$$\mathrm{Qgd}^{t}_{i,d,k} - \Delta d_d \mathcal{B}\mathrm{gd}_{i,d,k} \leq \mathrm{Qgd}^{t,s}_{i,d,k} \leq \mathrm{Qgd}^{t}_{i,d,k} + \Delta d_d \mathcal{B}\mathrm{gd}_{i,d,k} \qquad \forall\ d \in D^C \tag{2.11e}$$

When there is a contingency for a discrete resource, all continuous resources can adjust their power generation within certain limits defined by the ramp factor for those resources. Constraints (2.12a) and (2.12b) ensure that the ramping for continuous resources is within ramp limits (Δc_c) and is applied for all $i \in N, c \in C, t \in T, s \in S$.

$$\mathrm{Pgc}^{t}_{i,c} - \Delta c_c \mathcal{B}\mathrm{gc}_{i,c} \leq \mathrm{Pgc}^{t,s}_{i,c} \leq \mathrm{Pgc}^{t}_{i,c} + \Delta c_c \mathcal{B}\mathrm{gc}_{i,c} \tag{2.12a}$$

$$\mathrm{Qgc}^{t}_{i,c} - \Delta c_c \mathcal{B}\mathrm{gc}_{i,c} \leq \mathrm{Qgc}^{t,s}_{i,c} \leq \mathrm{Qgc}^{t}_{i,c} + \Delta c_c \mathcal{B}\mathrm{gc}_{i,c} \tag{2.12b}$$

2.3.13 Continuous Resources Contingency

Similar to discrete resource contingencies, continuous resource contingencies are modeled using constraints (2.13a). The indexes in constraints (2.13a) i, c, and t correspond to the contingent scenario s and generator c at node i that is faulted during time period t. Constraint (2.13b) sets the upper limit for the power generation by the continuous resource during contingency s and is applied for all $i \in N, t \in T, c \in C, s \in S$.

$$\mathrm{Pgc}_{i,c}^{t,s} = 0, \quad \mathrm{Qgc}_{i,c}^{t,s} = 0 \tag{2.13a}$$

$$\mathrm{Pgc}_{i,c}^{t,s} \leq \mathrm{Pgc}_{i,c}^{\max}, \quad \mathrm{Qgc}_{i,c}^{t,s} \leq \mathrm{Qgc}_{i,c}^{\max} \tag{2.13b}$$

2.4 Algorithms

2.4.1 Base Algorithm

The first algorithm solves the whole model using a commercially available solver, Gurobi V6.5.0.

2.4.2 Scenario-based Decomposition Algorithm

We adopt a scenario-based decomposition (SBD) methodology whereby "scenarios" are added to the model one by one based on certain conditions. A scenario and contingency are used synonymously in our description of the SBD algorithm. Unrestricted shedding variables for the N-1 model, ($Pns_{i,t}^{s}$) and ($Qns_{i,t}^{s}$), identify the scenarios that cause infeasibility. The values of these variables are used to decide which scenario should be added to the model. The pseudo-code for the SBD algorithm is explained in Algorithm 1.

In the SBD algorithm, M denotes the mathematical model that is to be solved. Initially, M is the base model without N-1 security constraints, (Here, M consists of constraints (2.2a) through (2.7b)). A sub-problem ($SP1$) is defined for each of the contingent scenarios, as the model which includes objective function defined in (2.8a), without (2.1a), all constraints for an N-1 security analysis, and values of the variables from base model that are realized after solving the model M. Here, the objective function for $SP1$ minimizes $\sum_{i \in N} \sum_{t \in T} \sum_{s \in S}(|Pns^s_{i,t}| + |Qns^s_{i,t}|)$ and includes constraints (2.9a) through (2.10c). The objective function for sub-problem ($SP1$) for each of the contingencies s is stored in a vector $S_{obj}(s)$. The value of $S_{obj}(s) = \sum_{i \in N} \sum_{t \in T}(|Pns^s_{i,t}|+|Qns^s_{i,t}|)\ \forall\, s \in S$. SBD is an exact algorithm whenever the sub-problems are feasibility problems. Here, the exactness criteria is met when $\max(S_{obj}) = 0$ in the optimal solution, i.e. the sub-problems reduce to feasibility problems.

Algorithm 1: Scenario-based decomposition

Define M as base model without the N-1 constraints ;
Define S_{obj} as the vector of size S ;
Create scenario set S, indexed by s, with all scenarios ;
while $max(S_{obj}) > 0$ *or* $S = \emptyset$ **do**
    Solve the model, M ;
    Get the values of base model decision variables, $\overline{x}$;
    for $s \in S$ **do**
        Solve sub-problem SP1 for scenario s using $\overline{x}$;
        Update $S_{obj}(s)$;
    end
    Set candidate scenario, s_c = index of $\max(S_{obj})$;
    Add N-1 constraints for scenario s_c to model M;
    Update scenario set $S = S \setminus s_c$;
    Set $S_{obj}(s_c) = 0$;
end

2.5 Numerical results

We used Clemson University's high performance computing resource, the Palmetto Cluster, which has Intel® Xenon® CPU X7542, 24 core processors @ 2.67 GHz and 172 GB RAM. The optimization model and algorithms were implemented using JuMP [28] and Gurobi 6.5.0.

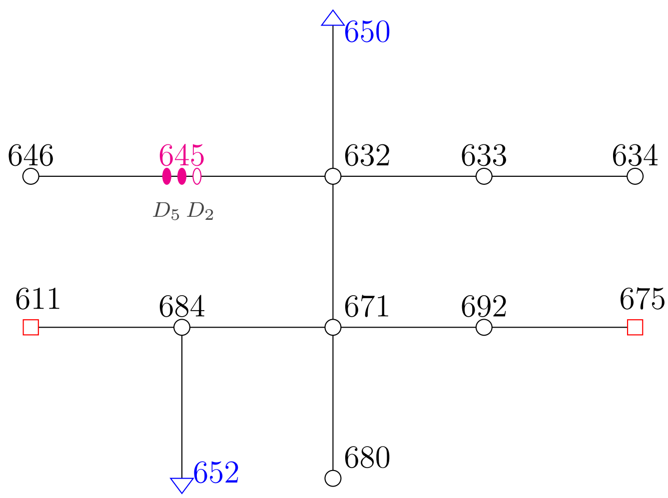

Figure 2.3: IEEE 13 node radial distribution test feeder

2.5.1 Case Study - IEEE 13

Our first case study uses the IEEE 13 node radial distribution test feeder [50], modified to use a positive-sequence representation (we use the constraint limits of [50]). This is illustrated in Fig. 2.3. In Fig. 2.3, red squares are nodes that have the ability to install continuous resources. Similarly, the blue triangular nodes can install discrete resources, while elliptical nodes (node 645) can accommodate both continuous and discrete resources. Demand data is for every 15 minutes (Δt=0.25 hours).

Demand data for this system is based on a New Mexico distribution utility.

The characteristics of the technology options available are provided in Table 2.3. We assume an efficiency of 95% for dispatched power $\leq 0.5 \times P_{rated}$ and 90% for dispatched power $> 0.5 \times P_{rated}$. We assume standby losses are 0.3 KW. The ramp-up and ramp-down rates are 200 KW per time-step.

TABLE 2.3: Characteristics of technology options

Tech Type	Fixed Cost ($)	Variable Cost ($/KW)	Operational Cost $aP^2 + bP + c$ ($)	Rated Power (Max, Min) (KW)
C1	100	300	$10P^2 + 5P + 2$	(100 , 0)
C2	200	250	$20P^2 + 10P + 4$	(100 , 0)
C3	250	200	$30P^2 + 15P + 8$	(100 , 0)
C4	300	150	$40P^2 + 20P + 10$	(100 , 0)
C5	350	100	$50P^2 + 25P + 5$	(100 , 0)
D1	200	0	$50P^2 + 25P + 6$	(250 , −250)
D2	100	0	$40P^2 + 20P + 5$	(275 , −250)
D3	250	0	$30P^2 + 15P + 4$	(300 , −250)
D4	300	0	$20P^2 + 10P + 3$	(225 , −250)
D5	350	0	$10P^2 + 5P + 2$	(200 , −250)

2.5.1.1 Base Algorithm

The solution times for design horizons of 5, 10, 15, 20, 50 and 96 time periods for the base algorithm are shown in Fig. 2.4. The 96 period (24 hours) design horizon problem took 1.5 hours to complete on the Palmetto cluster.

2.5.1.2 SBD

In comparison with the base algorithm, SBD is able to solve the 96 period problem in roughly 18 minutes (Fig. 2.4), a factor of 5× speedup. For this case study, the SBD approach is more efficient than solving the entire problem using commercial solvers.

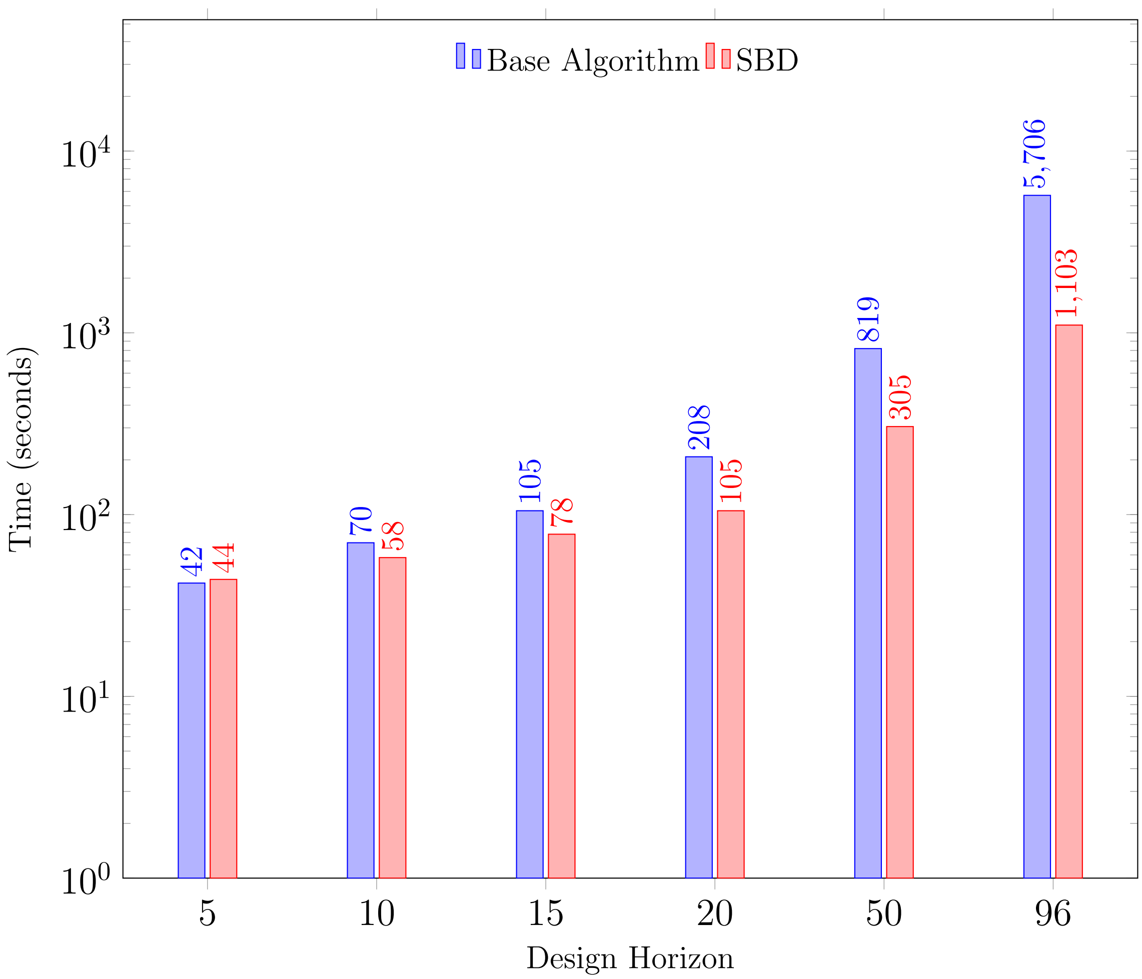

Figure 2.4: Results for the base algorithm and SBD

In this test case, devices D2 and D5 were installed at node 645. D5 is used more often than D2, due to its lower operational cost. The relative cost of N-1 security is provided in Fig. 2.5. Most of the difference in cost is due to dispatching D2 at higher levels to ensure N-1 feasibility.

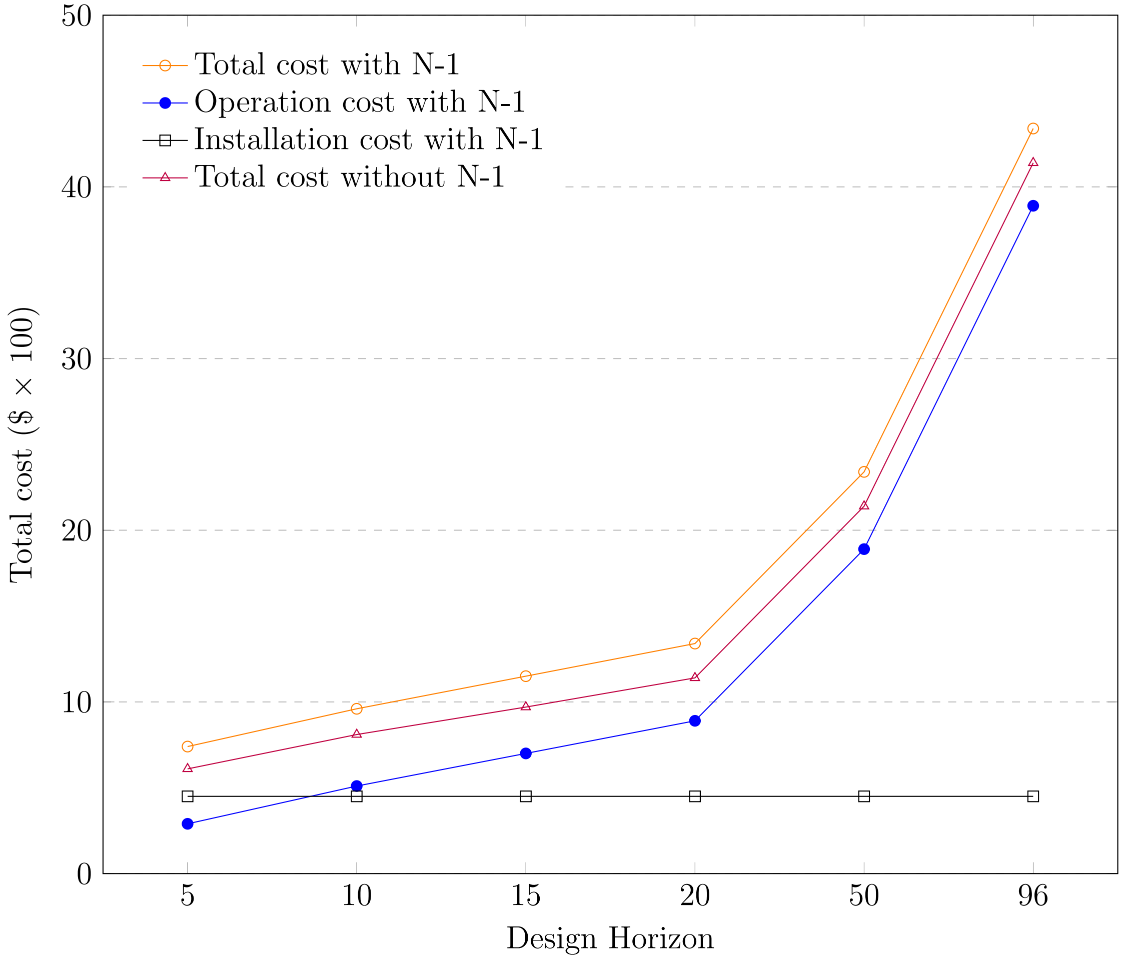

Figure 2.5: Total cost for each time period

2.5.2 Case Study - Alaskan Microgrid

We next present results based on the distribution circuits of a remote community in Alaska which was developed in [66]. There are 19 nodes in the network, whose schematic diagram is shown in Fig. 2.6. Node 1 has four generators and Node 3 has a wind generation unit. We ran the model with options to install generators at nodes 6, 8, 10, 14, and 18. These are nodes with critical loads including a hospital, airport, correctional center, gas station, and high school).

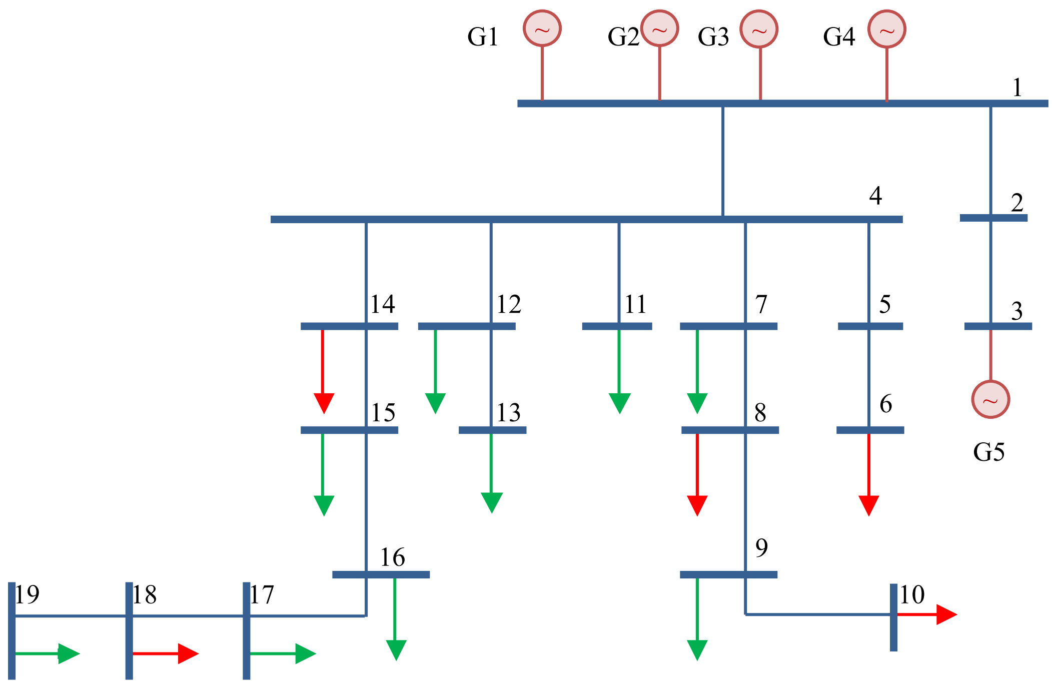

Figure 2.6: Schematic diagram of a remote community in Alaska

The characteristics of the technology options are provided in Table 2.4. We used the same efficiencies as in the IEEE case. The ramp-up and ramp-down rates were set to 190 KW for D1 and 500 KW for the rest. Details of the full model are available upon request.

We ran the model for 5, 10, 15, 20, 30, 50, and 96 period design horizons with the base model and the SBD algorithm. The solution times for various design horizons are shown in Fig. 2.7. Interestingly, the base algorithm slightly outperforms

TABLE 2.4: Characteristics of technology options for Alaskan microgrid

Tech Type	Fixed Cost ($)	Variable Cost ($/KW)	Operational Cost $aP2 + bP + c$ ($)	Rated Power (Max, Min) (KW)
D1	200	0	$50P^2 + 25P + 6$	(200 , 0)
D2,D3,D4,D5	500	0	$60P^2 + 20P + 5$	(1500 , 0)

the SBD algorithm. In this case, none of the contingencies dominate the other, so all contingencies must be added (see Table 2.5). In this worst case for SBD, SBD becomes the base algorithm with extra computational overhead. However, this overhead was relatively small, suggesting that the potential benefits of SBD outweigh the risk of this behavior. An interesting area of future work considers enhancements to SBD to avoid this situation.

TABLE 2.5: Number of scenarios added by SBD

Case Study	Base Algorithm	SBD
IEEE 13	18	3
Alaskan Microgrid	7	7

Once again, the dispatch was adjusted to satisfy contingency constraints. The new dispatch reduces the power output from the generators installed at node 8 and 14 and increases the dispatch from all other generators. The overall increase in cost for this increased dispatch due to contingencies is $195k. This confirms the importance of including N-1 security as discussed in [66].

2.5.3 Sensitivity Analysis

It is important to understand the impact of including N-1 security constraints and component efficiencies (as compared to the prior models of Table 2.1). Table 2.6

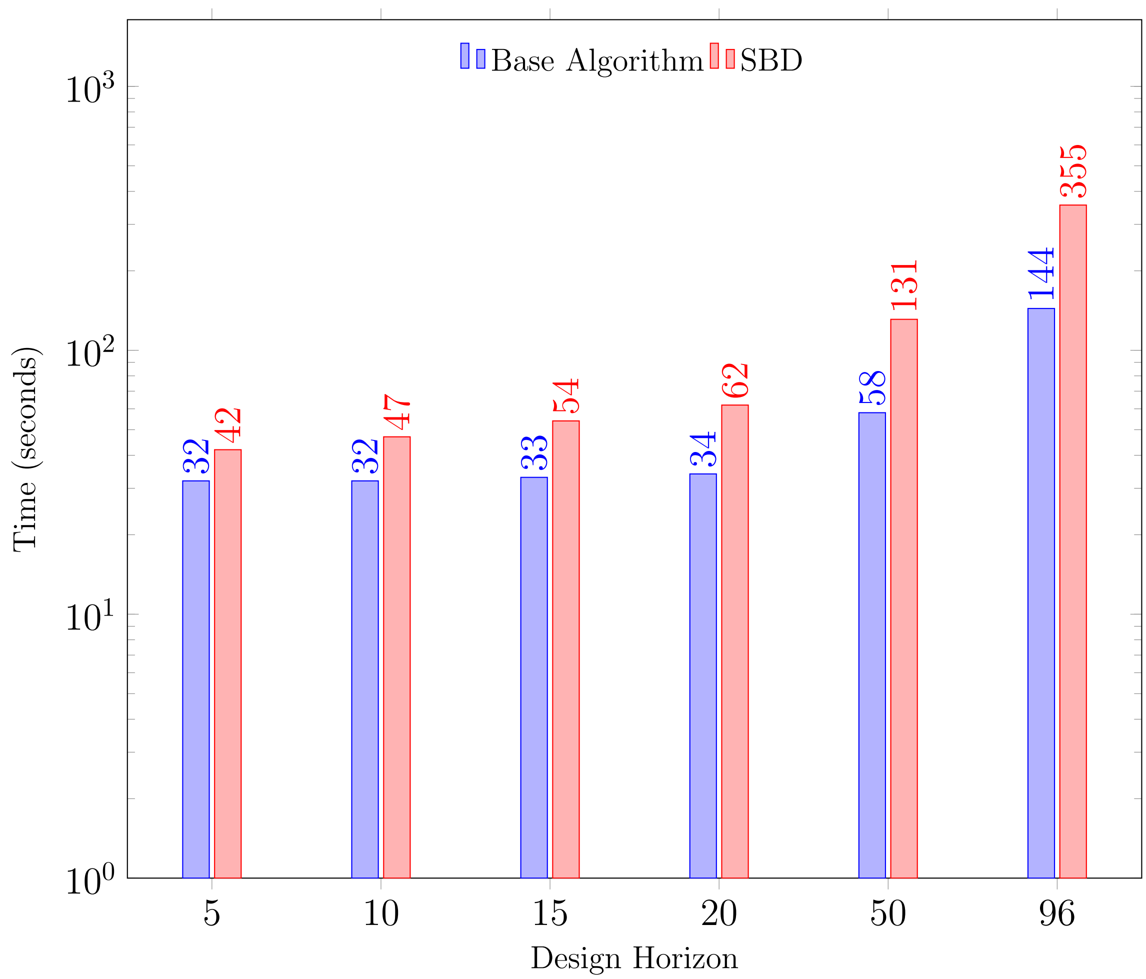

Figure 2.7: Solution time for Alaskan microgrid model using SBD

shows the impacts of introducing these modeling details to the IEEE 13 bus model. As expected, the computation time increases dramatically when N-1 security constraints are included in the model. Moreover, both efficiencies and N-1 can considerably alter the solutions themselves. For example, when efficiencies are not modeled the total cost is reduced because generation is not required to cover the losses associated with storage. In short, there are three key observations contained in Table 2.6. First, the sensitivity of the design choices are tied to whether or not N-1 contingencies are included in the model. Including these constraints forces the inclusion of additional resources. This result is common to both our model and prior work that has included N-1 constraints. Second, the inclusion of efficiencies significantly alters the operating cost (as much as 25%). Third, we note that the solutions are insensitive to the network flow, indicating, at least on this problem, that voltages are not an issue during the contingencies. We conjecture that a careful consideration of the voltage profiles during contingencies will provide insight on the importance of including these constraints on other problems. Finally, it is important to note that we have also indicated models described by prior literature in the last column of the table.

We also performed a sensitivity analysis on the various combinations of technology resources that are available for investment. Table 2.7 considers solutions where discrete technology resources are available, continuous technology resources are available, and both are available. Interestingly, rows 1 and 3 have the same objective function and the same solution. Given the assumptions on the relative costs of the different resources, the discrete technologies are more desirable. When only continuous resources are allowed, the solution cost is considerably higher.

TABLE 2.6: Sensitivity Analysis

S.No	N-1	Efficiency	Power flow Model	Run time Seconds	Objective cost ($)	Min. Voltage (kV)	Max. Voltage (kV)	Solution	References
1	×	✓	*LinDistFlow*	57	4137.51	3.952	3.954	D5 at Node 652	
2	×	✓	Network Model	29	4137.51	3.952	3.952	D5 at Node 650	[77]
3	×	×	*LinDistFlow*	503	3385.23	4.16	4.37	D5 at Node 650	
4	×	×	Network Model	424	3385.23	3.952	3.952	D5 at Node 645	[86], [82], [67]
5	✓	✓	*LinDistFlow*	5705	4337.51	3.952	3.954	D5 and D2 at Node 645	This work
6	✓	✓	Network Model	1678	4337.51	3.952	3.952	D5 and D2 at Node 645	
7	✓	×	*LinDistFlow*	12143	3617.23	4.17	4.14	D5 and D2 at Node 645	
8	✓	×	Network Model	13467	3617.23	3.952	3.952	D5 and D2 at Node 645	[51]

TABLE 2.7: Sensitivity analysis with resource options

S.No	Continuous	Discrete	Objective function ($)	Run time (Sec.)
1	✓	✓	4337.5	5706
2	✓	×	12386.0	1042
3	×	✓	4337.5	59

TABLE 2.8: Gap for objective functions

Case Study	*LinDistFlow* ($)	*DistFlow* ($)	Gap (%)
IEEE 13	4337.51	4337.99	0.011
Alaskan Microgrid	66940641.76	68650106.97	2.490

2.5.4 Feasible Solution Recovery

It is also important to validate the solutions obtained using the approximate *LinDistFlow* equations. Here, we used the *DistFlow* equations from Baran and Wu [12] for validation. The installation choices and commitment choices are fixed by the *LinDistFlow* solution. Knitro is used to find a locally optimal dispatch solution based on *DistFlow*. A feasible solution was always found and a comparison of the objective values is shown in Table 2.8. Generally speaking, the solutions found using *LinDistFlow* are a good approximation of what is necessary when modeling the full physics of the system.

2.6 Conclusions

In this research, we develop a mathematical formulation for planning and operation of remote off-grid microgrids with N-1 security constraints and component efficiencies. We show that a scenario-based decomposition algorithm using a *LinDistFlow* approximation can effectively solve these problems based on results for a modified IEEE 13 bus and the Alaskan distribution feeder. The effectiveness of the approximation is validated with the full nonlinear ac physics. There remain a number of interesting future directions for this research. First, we need to scale this approach to model multiple days of potential demands corresponding to different usage requirements. Second, we have assumed a purely deterministic model of generation and future work will need to incorporate stochastic renewable resources (wind, solar), and the unscheduled flows associated with them [69]. Here, the probabilistic chance constraints of [89] are an attractive option. Third, resiliency criteria is also an important criteria to consider in the future. One possibility is to include criteria with constraints and additional planning scenarios as discussed in

[97]. Finally, we also need to include topology design choices into the model to better reflect planning choices faced by microgrid designers.

Acknowledgements This work is partially funded by the Office of Electricity Delivery and Energy Reliability, Distributed Energy Program of the U.S. Department of Energy under Contract No. DE-AC02-05CH11231 and Work Order M615000466. We also want to thank Dan Ton from the Office of Electricity Delivery and Energy Reliability for supporting our work.

Chapter 3

Optimal Design for Location, Capacity, Topology, and Operation of Resilient Off-grid Microgrids

3.1 Introduction

Within the United States and many other areas of the world, remote communities are disconnected from bulk transmission systems. Given the economic hurdles associated with connecting remote communities to these systems, many will remain isolated for the foreseeable future. However, it is important that these communities have the same level of reliability afforded by the bulk transmission systems [83]. To address this need, we develop an expansion planning model for off-grid microgrids that balances the costs of designing the system with the cost for operating these grids under N-1 reliability criteria. This model includes all three major decisions associated with the design and operation of off-grid microgrids: identifying the installation locations of power sources, determining capacity and power dispatch of those resources, and prescribing the network topology [59]. Though critically important, this problem is very difficult to solve given the non-convexities in discrete installation choices and power flow physics.

To address this problem, we adopt the mixed-integer, quadratically constrained, quadratic programming (MIQCQP) resource planning model of [19, 66] and modify it to support expansion planning with N-1 security constraints on lines. The resulting model is significantly more challenging to solve (the methods of [19, 66] do not directly scale to this problem) and we develop a rolling horizon (RH) algorithm to solve this problem. In short, the key contributions of this paper are:

- To the best of our knowledge, the first planning model of distribution systems with topology decisions and N-1 reliability on lines that includes nonlinear ac physics, time-extended operations, resource planning decisions, and power device efficiencies. We refer to this problem as the ac integrated resource planning problem for microgrids, or ACIRPM for short.
- An algorithm that efficiently solves this problem.
- A demonstration on real system data and empirical validation of the results.

3.2 Literature Review

The importance of topology designs in power systems are discussed extensively in many research papers. An earlier study of the investment and operation of multiple energy systems along with their topology is discussed in Bakken *et al.* [11]. The paper examines the design and operation of multiple energy carriers within a locality and considers suggestions for alternate locations that satisfy pre-defined future demands. The authors recommend ranking the installation of various energy carriers for a

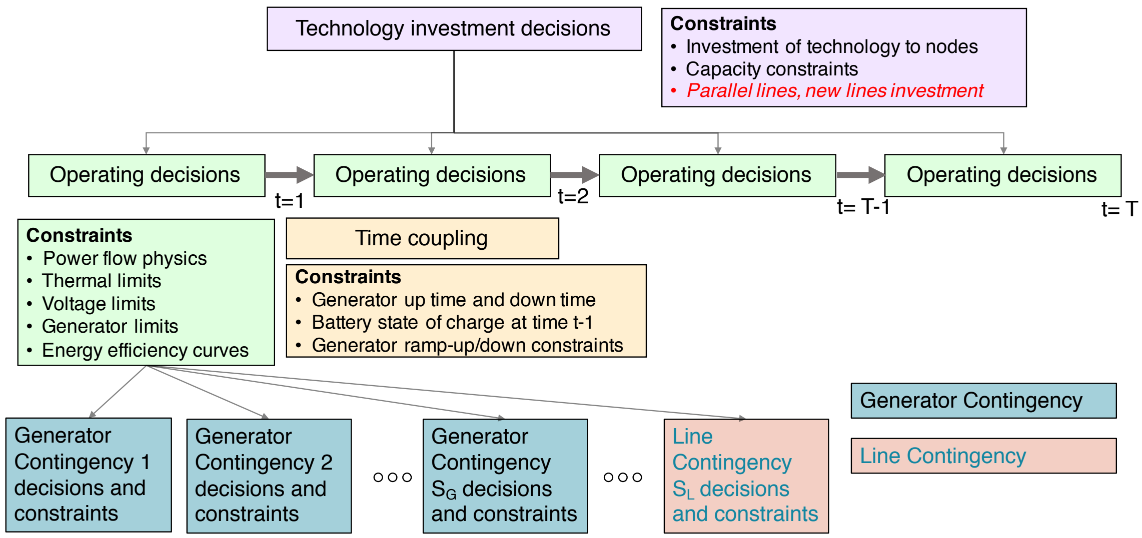

Figure 3.1: Modified flowchart of the microgrid resource planning model of [19]

defined time line. Their solution selects the network topology that minimizes the total cost of installation and operation. Even though Bakken *et al.* [11] considers topological design decisions, no contingency analysis was performed on the system. Furthermore, [25] studies an estimation for the vulnerability of an electric grid using topological analysis. The authors model cascading failures of power systems based on the dynamic load redistribution on the networks and observe that the system is high vulnerable when heavily loaded nodes are removed from the system.

In many places in the scientific literature, the optimization of microgrid topology design and operations is discussed as one of the main research needs in power systems, i.e. [78, 65]. This observation has driven a number of studies on how topology designs impact system security [4, 25, 11]. As noted by Lasseter *et al.* [58], typical microgrid architectures are organized in groups of radial feeders that are part of either a distribution network or independent, remote locations. Under these architectures, the removal of sets of nodes (network disruptions, generator breakdowns or line failures), can lead to cascading failures of these network. Given this observation, [4] considers the robustness of power systems from a topological perspective and verifies correlations between reliability and redundancy of network structure and emphasizes that a redundant network enhances reliability. In all of these papers, focus is placed on analyzing existing topology choices and these papers do not discuss the topological design of the network.

Some of the techniques for enhancing microgrid reliability using topological designs include interconnected microgrids and establishing network redundancy [33, 48, 100]. In terms of enhancing microgrid reliability through design, both [33] and [48] discuss interconnected microgrids. Erol-Kantarci *et al.* [33] discuss providing interconnection between microgrids to provide reliable networks, which can also help to increase the penetration of renewable energy in networked smart grids. Kahveci *et al.* [48] present a better topology layout using heuristics that employ clustering and graph theoretic methods. The authors discuss a heuristic approach to topology design for both "greenfield" sites and the augmentation of existing military distribution networks. The algorithm first identifies the minimum spanning tree between various nodes and then identifies various clusters that are electro-mechanically stable during islanding conditions. Unfortunately, these techniques may not be suitable for off-grid microgrids that cannot be connected to other microgrids. Zinchenko *et al.* [100] solve the transmission expansion planning problem with line redundancies as a two-path problem using a variant of Dijkstra's algorithm to find the shortest path. Their conclusion was that in order to design a resilient power system, redundancy may be the only option. Hence in our paper, we consider parallel, redundant lines to ensure that the network is N-1 secure for line contingencies. None of the previous research efforts consider N-1 security analysis on line contingencies as is the case in our study.

The most closely related work to this paper is found in [19, 66]. These papers develop a resource planning model for optimizing the placement generation resources to enforce N-1 generator reliability on microgrids. These papers also consider time-extended operations, power device efficiencies, and nonlinear ac physics. They do not consider expansion planning or N-1 reliability on lines. These two modeling details significantly increase the complexity of the problem and necessitate the need for new algorithmic approaches.

More generally speaking, the power engineering community has developed a number of techniques for solving problems with multiple time periods like ACIRPM. These methods include Benders decomposition [5], rolling horizon (RH) methods [76], graph partitioning [20], and branch-and-bound algorithms coupled with Lagrangian dual relaxation [38, 39]. Based on the strength of RH methods in industrial domains such as supply chain optimization [99] and recent strong results based on RH for operating microgrids [76], we developed an RH approach for solving the ACIRPM. Uniquely, we consider different approaches, such as scenario-based decomposition (SB), for solving the sub problems constructed by RH approaches.

The rest of the paper is organized as follows: Section II introduces the modified mathematical formulation for the resilient design and operation of off-grid microgrids along with N-1 security constraints on generators and lines. Section III presents a rolling horizon algorithm for solving the model efficiently and compares its results with scenario-based decomposition method. Numerical results on two case studies are discussed in Section IV. Finally, Section V presents conclusions and future directions of research.

3.3 Mathematical Formulation

In this section we present the ACIRPM model. The ACIRPM model combines expansion planning decisions with time extended operations, resource planning, efficiencies, and N-1 security criteria to optimize a microgrid for resilience.

3.3.1 Model Parameters and Variables

Sets

$\mathcal{N}$	set of nodes (buses), indexed by i
$\mathcal{E}$	set of existing edges (lines and transformers), indexed by e_{ij}. Each edge is assigned an arbitrary direction from a bus i to a bus j. ij is omitted when direction is not needed.
$\mathcal{E}_n$	set of new edges (lines and transformers), indexed by e_{ij}. Each edge is assigned an arbitrary direction from a bus i to a bus j. ij is omitted when direction is not needed.
$\mathcal{C}_i^C \subseteq \mathcal{C}$	set of continuous resources at bus i, indexed by c
$\mathcal{C}_i^{CB} \subseteq \mathcal{C}$	set of continuous resources with storage capabilities at bus i, indexed by c
$\mathcal{D}_i \subseteq \mathcal{D}$	set of discrete resources at bus i, indexed by d
$\mathcal{A}_i \subseteq \mathcal{A}$	set of resources at bus i, indexed by a
$\mathcal{E}_i^+$	set of existing and new edges connected to bus i and oriented from i, indexed by e
$\mathcal{E}_i^-$	set of existing and new edges connected to bus i and oriented to i, indexed by e
$\mathcal{K}_i$	set of slots at bus i, indexed by k_i
$\mathcal{T}$	set of time periods, indexed by t, numbered from 1 to $\|\mathcal{T}\|$
$\mathcal{C}$	set of continuous resources, indexed by c

$\mathcal{C}^D \subseteq \mathcal{C}$	set of continuous resources with discrete operation, indexed by c
$\mathcal{C}^C \subseteq \mathcal{C}$	set of continuous resources with continuous operation, indexed by c
$\mathcal{C}^B \subseteq \mathcal{C}^C$	set of continuous battery resources, indexed by c
$\mathcal{D}$	set of discrete resources, indexed by d
$\mathcal{D}^D \subseteq \mathcal{D}$	set of discrete resources with discrete operation, index by d
$\mathcal{D}^C \subseteq \mathcal{D}$	set of discrete resources with continuous operation, indexed by d
$\mathcal{A} = \mathcal{C} \cup \mathcal{D}$	set of all resources, indexed by a
Ω	set of scenarios for N-1 security analysis, indexed by ω

Parameters

f_a	fixed cost for resource $a \in \mathcal{A}$, (\$)
g_a	variable cost for resource $a \in \mathcal{A}$, (\$/MW)
$\kappa_{a,0}, \kappa_{a,1}, \kappa_{a,2}$	fixed, linear, and quadratic operational cost for resource $a \in \mathcal{A}$, (\$)
f_e	installation cost for line $e \in \mathcal{E}_n$, (\$)
$\overline{u}_d$, $\underline{u}_d$	minimum up-time and down-time for resource $d \in \mathcal{D}D$, (time-step)
$\overline{\gamma}_d$, $\underline{\gamma}_d$	ramp up and ramp down rate for resource $d \in \mathcal{D}$, (MW/time-step)
s_e	apparent power thermal limit on line $e \in \mathcal{E}$, (MVA)
lp_i^t, lq_i^t	Active and reactive power demand at bus $i \in \mathcal{N}$ at time $t \in \mathcal{T}$, $(\mathrm{MW}, \mathrm{MVAr})$
$\overline{pg}_a, \overline{qp}_a$	maximum active and reactive power generated by a resource $a \in \mathcal{A}$, $(\mathrm{MW}, \mathrm{MVAr})$
$\underline{pg}_a, \underline{qp}_a$	minimum active and reactive power generated by a resource $a \in \mathcal{A}$, (MW)

Γ_c	maximum energy storage capacity of the battery $c \in \mathcal{C}^B$, (MVA)
$\underline{v_i}, \overline{v_i}$	Squared voltage lower and upper bound at bus $i \in \mathcal{N}$, $((kV)^2)$
$\overline{s}_a$	maximum apparent power generated by resource $a \in \mathcal{A}$, (MVA)
l_a^p	Stand-by loss (y intercept) of a resource $a \in A$ for each piecewise function $p \in \{1, .., P\}$, (MW)
$[\eta_a^1 \dots \eta_a^p]$	Vector of piecewise marginal efficiencies of maximum rated power, (%)
$\mathrm{r}_e, \mathrm{x}_e$	Resistance and reactance of line $e \in \mathcal{E}$, $(k\Omega)$
Δt	duration of a time-step, (hr)
h_{i}	Maximum number of continuous resources at bus i
k_i	Maximum number of discrete resources at bus i, indexed by k_i

Binary Decision Variables: Discrete technology

x_d^t	active/inactive status for resource $d \in \mathcal{D}$ at time $t \in \mathcal{T}$
y_d^t	start-up status for resource $d \in \mathcal{D}$ at time $t \in \mathcal{T}$
w_d^t	shut-down status for resource $d \in \mathcal{D}$ at time $t \in \mathcal{T}$
b_d	status indicator if discrete resource $d \in D$ is built

Binary Decision Variables: Continuous technology

b_c	status indicator if continuous resource $c \in C$ is built

Continuous decision variables: Discrete technology

pg_d^t	ac active power generation during time $t \in \mathcal{T}$ for discrete resource $d \in \mathcal{D}$, (MW)

qg_d^t	ac reactive power generation during time $t \in \mathcal{T}$ for discrete resource $d \in \mathcal{D}$, (MVAr)
$\hat{pg}_d^t$	ac active power generation before losses during time $t \in \mathcal{T}$ for discrete resource $d \in \mathcal{D}$, (MW)

Continuous decision variables: Continuous technology

$\tilde{pg}_c, \tilde{qp}_c$	installed maximum active and reactive power generated by a resource $c \in \mathcal{C}$, (MW, MVAr)
$\tilde{s}_c$	installed maximum apparent power generated by resource $c \in \mathcal{C}$, (MVA)
pg_c^t, qg_c^t	ac apparent power generation during time $t \in \mathcal{T}$ for continuous resource $c \in \mathcal{C}$, (MW, MVAr)
$\hat{pg}_c^t$	ac active power generation before losses during time $t \in \mathcal{T}$ for continuous resource $c \in \mathcal{C}$, (MW)
ς_c^t	Energy stored (state of charge) in the continuous resource battery $c \in \mathcal{C}^B$ at time $t \in \mathcal{T}$, (MW-hr)

Continuous decision variables: Others

$\mathrm{p}_e^t, \mathrm{q}_e^t$	Active and reactive power flow though edge $e \in \mathcal{E}$ at time $t \in \mathcal{T}$, (MW, MVAr)
v_i^t	Squared voltage at node $i \in \mathcal{N}$ at time $t \in T$, $((kV)^2)$
$lp_i^{t,s}, lq_i^{t,\omega}$	apparent power slack at node $i \in \mathcal{N}$ at time $t \in T$ during contingency scenario $\omega \in \Omega$, (MW, MVAr)

Binary decision variables: Lines

b_e	status indicator if line $e \in \mathcal{E}_n$ is built

3.3.2 Objective Function

The objective function of the ACIRPM lexicographically minimizes load slack during the contingencies and then minimizes the total installation and operation cost of energy resources and the cost of installing new lines to enhance network resiliency (3.1a).

$$\min \Bigg\langle \; \Bigg(\sum_{i\in\mathcal{N}} \sum_{t\in\mathcal{T}} \sum_{\omega\in\Omega} (|lp^{\omega}_{i,t}| + |lq^{\omega}_{i,t}|) \Bigg),$$
$$\Bigg(\sum_{c\in\mathcal{C}} f_c b_c + \sum_{c\in\mathcal{C}\setminus\mathcal{C}^B} g_c \tilde{pg}_c + \sum_{c\in\mathcal{C}^B} g_c \tilde{s}_c \Bigg) + \sum_{d\in\mathcal{D}} f_d b_d \; + \sum_{e\in\mathcal{E}_n} f_e b_e +$$
$$\Bigg(\sum_{t\in T} \sum_{a\in\mathcal{A}} \big((\kappa_{a,2})(\hat{pg}^t_a)^2 + (\kappa_{a,1})(\hat{pg}^t_a) + (\kappa_{a,0})(b_a) \big) \Bigg) \; \Bigg\rangle \tag{3.1a}$$

3.3.3 Resource Planning

The constraints associated with the availability of resources are defined in equations (3.2a)-(3.2g). Here, equations (3.2a)-(3.2b) link the installed capacity of continuous resources to the build variable. Equation (3.2c) links the installed apparent power capacity of storage devices with the build variable. Similarly, equations (3.2f)-(3.2g) constrain the capacity limits for discrete resources. The number of continuous and discrete resources installed at a bus is constrained by equations (3.2d)-(3.2e).

$$pg^t_c \leq \tilde{pg}_c \leq b_c \overline{pg}_c \qquad \forall\, c \in \mathcal{C} \setminus \mathcal{C}^B, t \in \mathcal{T} \tag{3.2a}$$

$$qg^t_c \leq \tilde{qg}_c \leq b_c \overline{qg}_c \qquad \forall\, c \in \mathcal{C}, t \in \mathcal{T} \tag{3.2b}$$

$$\tilde{s}_c \leq b_c \overline{s}_c \qquad \forall\, c \in \mathcal{C}^B \tag{3.2c}$$

$$\sum_{c\in\mathcal{C}_i} b_c \leq h_i \qquad \forall\, i \in \mathcal{N} \tag{3.2d}$$

$$\sum_{d\in\mathcal{D}_i} b_d \leq k_i \qquad \forall\, i \in \mathcal{N} \tag{3.2e}$$

$$\underline{pg}_d b_d \leq \hat{pg}_d^t \leq \overline{pg}_d b_d \qquad \forall\, d \in \mathcal{D}^C, t \in \mathcal{T} \tag{3.2f}$$

$$\underline{qg}_d b_d \leq qg_d^t \leq \overline{qg}_d b_d \qquad \forall\, d \in \mathcal{D}^C, t \in \mathcal{T} \tag{3.2g}$$

3.3.4 Power Flow Physics

The physics of the ACIRPM are shown in equations (3.3a)-(3.3c), where the *LinDistFlow* equations (3.3c) of [36, 12] are used. Here, (3.3a)-(3.3b) model Kirchoff's Law and (3.3c) models Ohm's Law.

$$\sum_{a \in \mathcal{A}_i} pg_a^t - lp_i^t = \sum_{e \in \mathcal{E}_i^+} p_e^t - \sum_{e \in \mathcal{E}_i^-} p_e^t \qquad \forall\, i \in \mathcal{N}, t \in \mathcal{T} \tag{3.3a}$$

$$\sum_{a \in \mathcal{A}_i} qg_a^t - lq_i^t = \sum_{e \in \mathcal{E}_i^+} q_e^t - \sum_{e \in \mathcal{E}_i^-} q_e^t \qquad \forall\, i \in \mathcal{N}, t \in \mathcal{T} \tag{3.3b}$$

$$v_j^t = v_i^t - 2(\mathrm{r}_e \mathrm{p}_e^t + \mathrm{x}_e \mathrm{q}_e^t) \qquad \forall\, e_{ij} \in \mathcal{E}, t \in \mathcal{T} \tag{3.3c}$$

3.3.5 Physical Limits

The physical limits of the ACIRPM are shown in equations (3.4a)-(3.4b). Equation (3.4a) places thermal limits on lines and equation (3.4b) places voltage magnitude limits on buses.

$$(\mathrm{p}_e^t)^2 + (\mathrm{q}_e^t)^2 \leq (s_e)^2 \qquad \forall\, e \in \mathcal{E}, t \in \mathcal{T} \tag{3.4a}$$

$$\underline{\mathrm{v}_i} \leq v_i^t \leq \overline{\mathrm{v}_i} \qquad \forall\, i \in \mathcal{N}, t \in \mathcal{T} \tag{3.4b}$$

3.3.6 Generator Limits

Equations (3.5a)-(3.5i) model the operating limits of resources defined as discrete generators (i.e. diesel generators). The connection between a generator's on/off status and its start-up and shutdown time are modeled with equations (3.5a)-(3.5c) . Equations (3.5d)-(3.5e) link active and reactive power dispatch with the generator's status. Generator operating characteristics like minimum up-time, minimum down-time, ramp-up time, and ramp-down time are constrained using equations (3.5f)-(3.5g). We model the boundary conditions of uptime and downtime using $\alpha_d = \rho \in \mathcal{T} : t - \overline{u}_d + 1 \leq \rho \leq t$ and $\zeta_d = \rho \in \mathcal{T} : t - \underline{u}_d + 1 \leq \rho \leq t$ respectively.

$$x_d^t \leq b_d \qquad \forall\, d \in \mathcal{D}^D, t \in \mathcal{T} \tag{3.5a}$$

$$x_d^t = x_d^{t-1} + y_d^t - w_d^t \qquad \forall\, d \in \mathcal{D}^D, t \in \mathcal{T} \tag{3.5b}$$

$$y_d^t + w_d^t \leq 1 \qquad \forall\, d \in \mathcal{D}^D, t \in \mathcal{T} \tag{3.5c}$$

$$\underline{pg}_d x_d^t \leq \hat{pg}_d^t \leq \overline{pg}_d x_d^t \qquad \forall\, d \in \mathcal{D}^D, t \in \mathcal{T} \tag{3.5d}$$

$$\underline{qg}_d x_d^t \leq \hat{qg}_d^t \leq \overline{qg}_d x_d^t \qquad \forall\, d \in \mathcal{D}^D, t \in \mathcal{T} \tag{3.5e}$$

$$\sum_{\rho \in \alpha_d} y_d^\rho \leq x_d^t \qquad \forall\, d \in \mathcal{D}^D, t \in \mathcal{T} \tag{3.5f}$$

$$\sum_{\rho \in \zeta_d} w_d^\rho \leq 1 - x_d^t \qquad \forall\, d \in \mathcal{D}^D, t \in \mathcal{T} \tag{3.5g}$$

$$\overline{\gamma}_d \geq pg_d^t - pg_d^{t-1} - \overline{pg}_d y_d^t \qquad \forall\, d \in \mathcal{D}^D t \in \mathcal{T} \tag{3.5h}$$

$$\underline{\gamma}_d \geq pg_d^{t-1} - pg_d^t - \overline{pg}_d w_d^t \qquad \forall\, d \in \mathcal{D}^D t \in \mathcal{T} \tag{3.5i}$$

3.3.7 Battery Limits

Equations (3.6a)-(3.6c) model the operating limits of resources defined as batteries. Equation (3.6a) constrains the apparent power of batteries. The charging and discharging of batteries are modeled using equations (3.6b).

$$(pg_c^t)^2 + (qg_c^t)^2 \leq (\tilde{s}_c)^2 \qquad \forall\, c \in \mathcal{C}^B, t \in \mathcal{T} \tag{3.6a}$$

$$\varsigma_c^t = \varsigma_c^{t-1} - \hat{pg}_c^t \Delta t \qquad \forall\ c \in \mathcal{C}^B, t \in \mathcal{T} \tag{3.6b}$$

$$0 \leq s_c^t \leq \tilde{s_c} \qquad \forall\ c \in \mathcal{C}^B, t \in T \tag{3.6c}$$

3.3.8 Efficiencies

Component efficiencies are defined using a piece-wise linear functions (p) defined in constraints (3.7a) - (3.7c). Our models have four linear functions for each component.

$$pg_c^t \leq \eta_c^p \hat{pg}_c^t + b_c l_c^p \qquad \forall\ c \in \mathcal{C}, t \in \mathcal{T}, p \tag{3.7a}$$

$$pg_d^t \leq \eta_d^p \hat{pg}_d^t + x_d^t l_d^p \qquad \forall\ d \in \mathcal{D}^C, t \in \mathcal{T}, p \tag{3.7b}$$

$$pg_d^t \leq \eta_d^p \hat{pg}_d^t + b_d l_d^p \qquad \forall\ d \in \mathcal{D}^D, t \in \mathcal{T}, p \tag{3.7c}$$

3.3.9 Expansion Planning

On/off constraints are used to model thermal limits (3.8a) and Ohm's laws (3.8b)-(3.8c) for new lines. Here $M = \overline{v_i} - \underline{v_i}$.

$$(p_e^t)^2 + (q_e^t)^2 \leq b_e * (s_e)^2 \qquad \forall e \in \mathcal{E}_n, t \in \mathcal{T} \tag{3.8a}$$

$$v_j^t - v_i^t \geq -2(r_e p_e^t + x_e q_e^t) - M(1 - b_e) \qquad \forall e_{ij} \in \mathcal{E}_n, t \in \mathcal{T} \tag{3.8b}$$

$$v_j^t - v_i^t \leq -2(r_e p_e^t + x_e q_e^t) + M(1 - be) \qquad \forall e_{ij} \in \mathcal{E}_n, t \in \mathcal{T} \tag{3.8c}$$

3.3.10 Generator Contingencies

Each generator contingency replicates equations (3.2a)-(3.8c) on subsets of $\mathcal{C}$ and $\mathcal{D}$. The subsets remove the generators that are outaged in the contingency.

Equations (3.3a) and (3.3b) are replaced with their load slack equivalents.

$$\sum_{a \in \mathcal{A}_i} pg_a^{t,\omega} - lp_i^t - lp_i^{t,\omega} = \sum_{e \in \mathcal{E}_i^+} p_e^{t,\omega} - \sum_{e \in \mathcal{E}_i^-} p_e^{t,\omega} \qquad \forall\, i \in \mathcal{N}, t \in \mathcal{T}, \omega \in \Omega \tag{3.9a}$$

$$\sum_{a \in \mathcal{A}_i} qg_a^{t,\omega} - lq_i^t - lq_i^{t,\omega} = \sum_{e \in \mathcal{E}_i^+} q_e^{t,\omega} - \sum_{e \in \mathcal{E}_i^-} q_e^{t,\omega} \qquad \forall\, i \in \mathcal{N}, t \in \mathcal{T}, \omega \in \Omega \tag{3.9b}$$

3.3.11 Line Contingencies

Each line contingency replicates equations (3.2a)-(3.8c) on subsets of $\mathcal{E}$ and $\mathcal{E}_n$. The subsets remove the lines that are outaged in the contingency. Equations (3.3a) and (3.3b) are replaced the same as generator contingencies.

3.4 Algorithms

3.4.1 Base Algorithm

We define the base algorithm as an approach that formalizes the entire model as a single input to the commercial solver Gurobi 7.0.1 [41]. We use this approach as a comparison point.

3.4.2 Scenario-based Decomposition (SBD) Algorithm

The SBD algorithm was first applied to microgrid resiliency problems in Chalil Madathil *et al.* [19] where it was shown to have considerable computational advantages. On these problems, SBD converges to the global optimal and we use it as another comparison point for our approach. For completeness, the SBD algorithm is outlined in Algorithm 2. SBD first relaxes the N-1 contingency constraints (model $\mathcal{M}_\emptyset$). Each N-1 contingency (scenario) is then solved given the resource and expansion planning decisions of the solution to $\mathcal{M}_{\emptyset}$. The constraints of the contingency that requires the most load slack is then added as part of the constraint set. The algorithm terminates when all contingencies are added or there is no load slack.

Algorithm 2: Scenario-based decomposition

Create scenario set S, indexed by ω, with all N-1 scenarios ;
Define S_{obj} as a vector of size S ;
while $max(S_{obj}) > 0$ *or* $S = \emptyset$ **do**
  Solve the model, $\mathcal{M}_{\Omega \setminus S}$;
  Get the values of base model decision variables, $\overline{x}$;
  for $\omega \in S$ **do**
    Solve sub-problem for scenario ω using $\overline{x}$;
    Update $S_{obj}(\omega)$;
  end
  Select scenario, $\omega = \arg\max_S S_{obj}(\omega)$;
  Update scenario set $S = S \setminus \omega$;
  Set $S_{obj}(\omega) = 0$;
end

3.4.3 Rolling Horizon Algorithm

In our initial computational experiments we found that the ACIRPM was computationally very challenging for both exact methods. Here, we discuss our rolling horizon (RH) heuristic that decomposes the ACIRMP into a sequence of smaller problems. Each sub problem considers a limited number of time periods. This heuristic was developed to address the scaling issues associated with these exact methods. Each sub problem of the RH is solved using one of these exact methods.

The RH algorithm is defined by three parameters, the scheduling horizon $T^s = |\mathcal{T}|$, a prediction horizon $\mathcal{T}^p$, and a control horizon $\mathcal{T}^c$. The scheduling horizon defines the full length of the ACIRMP. The prediction horizon controls the size of the sub problems that are solved, and the control horizon determines how much of the sub problem solution is executed. More formally, let σ_τ denote the solution to an ACIRMP $\mathcal{T}^c$ problem starting at time τ and let $\sigma_\tau(\cdot)$ denote the variable assignment of $\cdot$ in solution σ_τ. We can then recursively define the $\mathcal{T}^c$ problem, $\mathcal{M}^\tau$, as $\mathcal{M}$ where $T = \tau + \mathcal{T}^p$ and the following extra constraints.

$$b_c \geq \sigma_{\tau-\mathcal{T}^c}(b_c) \qquad \forall\, i \in \mathcal{N}, c \in \mathcal{C} \tag{3.10a}$$

$$b_d \geq \sigma_{\tau-\mathcal{T}^c}(b_d) \qquad \forall\, i \in \mathcal{N}, d \in \mathcal{D}^D, k \in K_i \tag{3.10b}$$

$$b_e \geq \sigma_{\tau-\mathcal{T}^c}(b_e) \qquad \forall\, ij \in \mathcal{E} \cup \mathcal{E}_n \tag{3.10c}$$

$$\tilde{pg}_c \geq \sigma_{\tau-\mathcal{T}^c}(\tilde{pg}_c) \;\;,\;\; \tilde{qg}_c \geq \sigma_{\tau-\mathcal{T}^c}(\tilde{qg}_c) \qquad \forall\, i \in \mathcal{N}, c \in \mathcal{C} \tag{3.10d}$$

These constraints are used to enforce consistency of installation decisions between $\mathcal{T}^c$ problems. Similarly, we also add constraints that enforce consistency in operation between $\mathcal{T}^c$ problems.

$$x_d^\tau = \sigma_{\tau-\mathcal{T}^c}(x_d^{\tau-1}) + y_d^\tau - w_d^\tau \qquad \forall\, d \in \mathcal{D}^D \tag{3.11a}$$

$$\sum_{\rho \in \alpha_d} y_d^\rho \leq x_d^t \qquad \forall\, d \in \mathcal{D}^D, t \in \mathcal{T} \tag{3.11b}$$

$$\sum_{\rho \in \zeta_d} w_d^\rho \leq 1 - x_d^t \qquad \forall\, d \in \mathcal{D}^D, t \in \mathcal{T} \tag{3.11c}$$

$$x_d^t = \begin{cases} 1, & \forall\, t \in [\tau, \tau + \overline{u}_d - \tilde{t}] \text{ , if } \sigma_{\tau-\mathcal{T}^c}(y_d^{\tilde{t}}) = 1 \\ 0, & \forall\, t \in [\tau, \tau + \underline{u}_d - \tilde{t}] \text{ , if } \sigma_{\tau-\mathcal{T}^c}(w_d^{t}) = 1 \end{cases} \tag{3.11d}$$

$$\overline{\gamma}_d \geq \sigma_{\tau-\mathcal{T}^c}(pg_d^{\tau-1}) - pg_d^\tau \qquad \forall\, d \in \mathcal{D}^D \tag{3.11e}$$

$$\underline{\gamma}_d \geq pg_d^\tau - \sigma_{\tau-\mathcal{T}^c}(pg_d^{\tau-1}) \qquad \forall\, d \in \mathcal{D}^D \tag{3.11f}$$

Constraints (3.11a) uses generator on/off status in $\sigma_{\tau-\mathcal{T}^c}$ as a boundary condition. We update the minimum value for the up-time and downtime as $\zeta_d =$

$\max(t - \overline{u}_d + 1, \min(\mathcal{T}^p))$ and $\alpha_d = \max(t - \underline{u}_d + 1, \min(\mathcal{T}^p))$ respectively, for use in constraints (3.11b) and (3.11c). The boundary condition should also ensure the proper calculation of minimum generator up-time and down-time. Let $\tilde{t}$ denotes the time instant a generator is turned on during its operation ($\sigma_{\tilde{t}}(y_d^t) = 1$). Then the value of $x_d^t = 1$ must be set for all time-steps until the minimum up-time criteria. This is enforced by (3.11d). Similarly, minimum down-time criteria is enforced by checking the value of $\sigma_{\tilde{t}}(w_d^t) = 1$. Finally, constraints (3.11e) and (3.11f) link the ramp-up and ramp-down rates between two adjacent time-steps.

Constraints are also added that enforce consistency in operation of batteries in $\mathcal{T}^c$ problems. Constraints (3.12a) ensure that the value of charge is carried forward from the previous iterations starting from time-step $\tau - \mathcal{T}^c$.

$$\varrho_c^\tau = \sigma_{\tau-\mathcal{T}^c}(\varrho_c^{\tau-1}) - pg_c^\tau \Delta t \qquad \forall\ c \in \mathcal{C}_i^{CB}, \tag{3.12a}$$

The pseudo-code for our RH is given in Algorithm 3 and a schematic diagram of the algorithm is presented in Fig. 3.2.

Algorithm 3: Rolling horizon algorithm

```
while τ ≤ T do
    Warm start M^τ with σ_{τ−T^c};
    σ_τ ← Solve M^τ ;
    τ ← τ + T^c ;
end
```

Each iteration uses the solution $\sigma_{\tau-\mathcal{T}^c}$ to *warm start* [41] the solver used to solve M^τ The *warm start* initializes the assignment of variables in M^τ with the assignments of those variables in $\sigma_{\tau-\mathcal{T}^c}$ (where these is overlap).

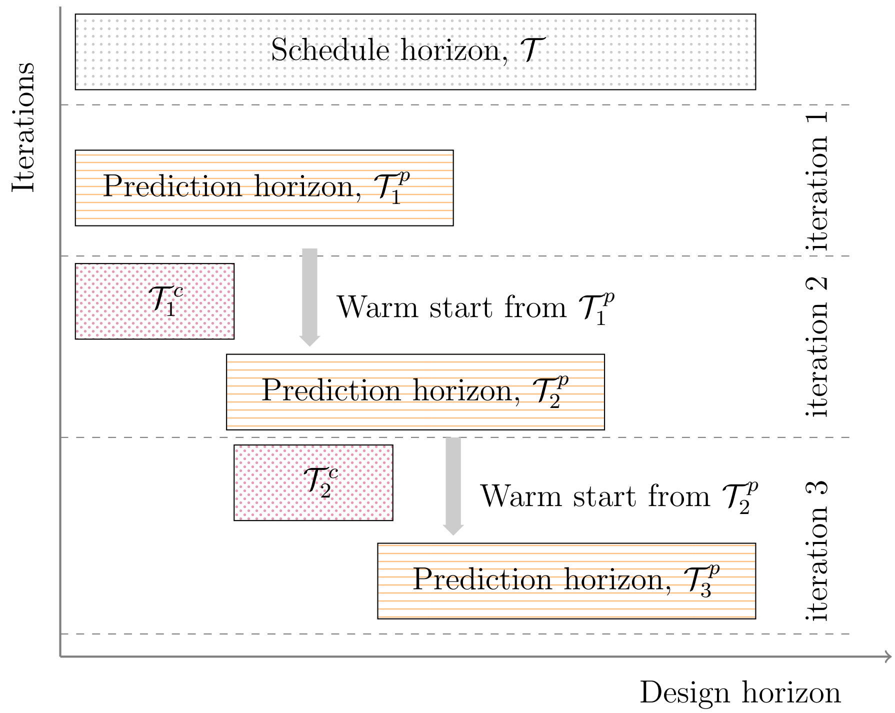

Figure 3.2: Schematic diagram for rolling horizon

3.5 Numerical Results

The numerical results were performed using a Microsoft Windows® Server 2016 with an Intel® Core™ i7-6950X CPU @ 3.00 GHz processor with 10 cores and 128 GB RAM. The algorithms are modeled using JuMP in Julia [28] and use Gurobi V7.0.1 to solve the QPs. We test the performance of the proposed algorithm and validate the model on an adapted version of the IEEE 13 node test feeder [50] and a real microgrid from Alaska.

3.5.1 Case Study 1: IEEE 13 Node Test Feeder

The original IEEE 13 node test feeder has 13 nodes and 12 lines (black solid lines in Figure 3.3). For this paper the network is modified as follows. Continuous resources (C_1 through C_5) can be installed at nodes 611 and 675. Discrete resources

(D_1 through D_5) can be installed at nodes 650 and 652. Both types of resources can be installed at node 645. The load for this system is based on data from a New Mexico distribution utility. Demand is added at all nodes and for all time-steps except for nodes 633, 650, 680, 684, and 692. These nodes have zero demand during the entire design horizon. The installation and operational costs for all resources in Table 3.2.

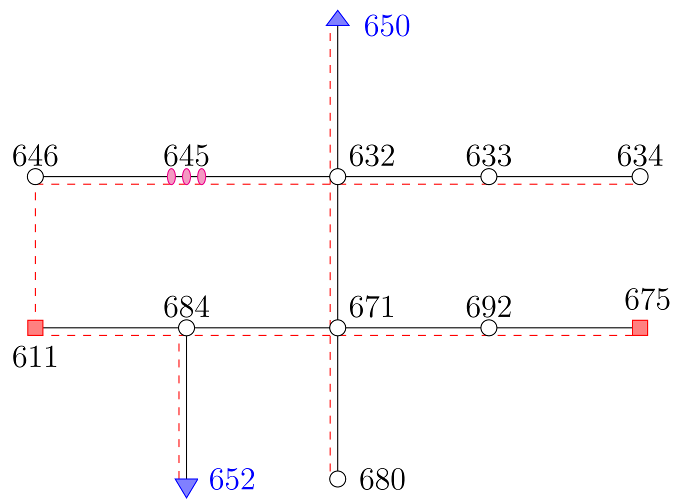

Figure 3.3: IEEE 13 node radial distribution test feeder with parallel lines. Black lines denote existing lines and red dashed lines denote possible expansions.

Expansion decisions for this network include parallel lines for all 12 existing lines and new lines between nodes 611 and 646 (parallel and new lines are marked as dotted red lines in Figure 3.3). The cost of installing parallel lines and new lines is $1000 per line. Physical characteristics of the lines are provided in Chalil Madathil *et al.* [19] and [50]. The design decision is provided for every 15 minutes and hence the number of time points is 96 for a day's problem. This network has 18 possible generator contingencies and 25 possible line contingencies.

TABLE 3.2: Characteristics of technology options for IEEE 13 Network

Tech Type	Fixed Cost ($)	Variable Cost ($/KW)	Operational Cost aP^2+bP+c ($)	Rated Power (Max, Min) (KW)
C_1	10000	300	$10P^2+5P+2$	(100 , 0)
C_2	20000	250	$20P^2+10P+4$	(100 , 0)
C_3	25000	200	$30P^2+15P+8$	(100 , 0)
C_4	30000	150	$40P^2+20P+10$	(100 , 0)
C_5	35000	100	$50P^2+25P+5$	(100 , 0)
D_1	20000	0	$50P^2+25P+6$	(250 , −250)
D_2	10000	0	$40P^2+20P+5$	(275 , −250)
D_3	25000	0	$30P^2+15P+4$	(300 , −250)
D_4	30000	0	$20P^2+10P+3$	(225 , −250)
D_5	35000	0	$10P^2+5P+2$	(200 , −250)

3.5.1.1 Recommended solution for 96 Design Horizon Problem

In this model, the optimal solution includes the installation of D_2 generators at nodes 650 and 652. The optimal solution also includes parallel lines between nodes 632 - 634, 671 - 675, and 611 - 646. In contrast, without expansion options, the solution is forced to build generators at 611, 645, 652, and 675.

3.5.1.2 Solution Time

Figure 3.4 evaluates the efficiency and effectiveness of our RH approach. This figure shows the computation time and solution quality of the two exact methods and RH for design horizons of 5, 10, 15, 20, 50, and 96. Each algorithm had a time limit of 24 hours. In all cases, the RH solution matches the solution found by the exact method. However, in both the SBD and base algorithm timed out in the 96 horizon case. The base algorithm found a feasible solution with a 98.% optimal gap after 24-hour time limit. The best RH was able to solve this same problem in 231 seconds.

For this particular problem instance, the base algorithm was able to find an

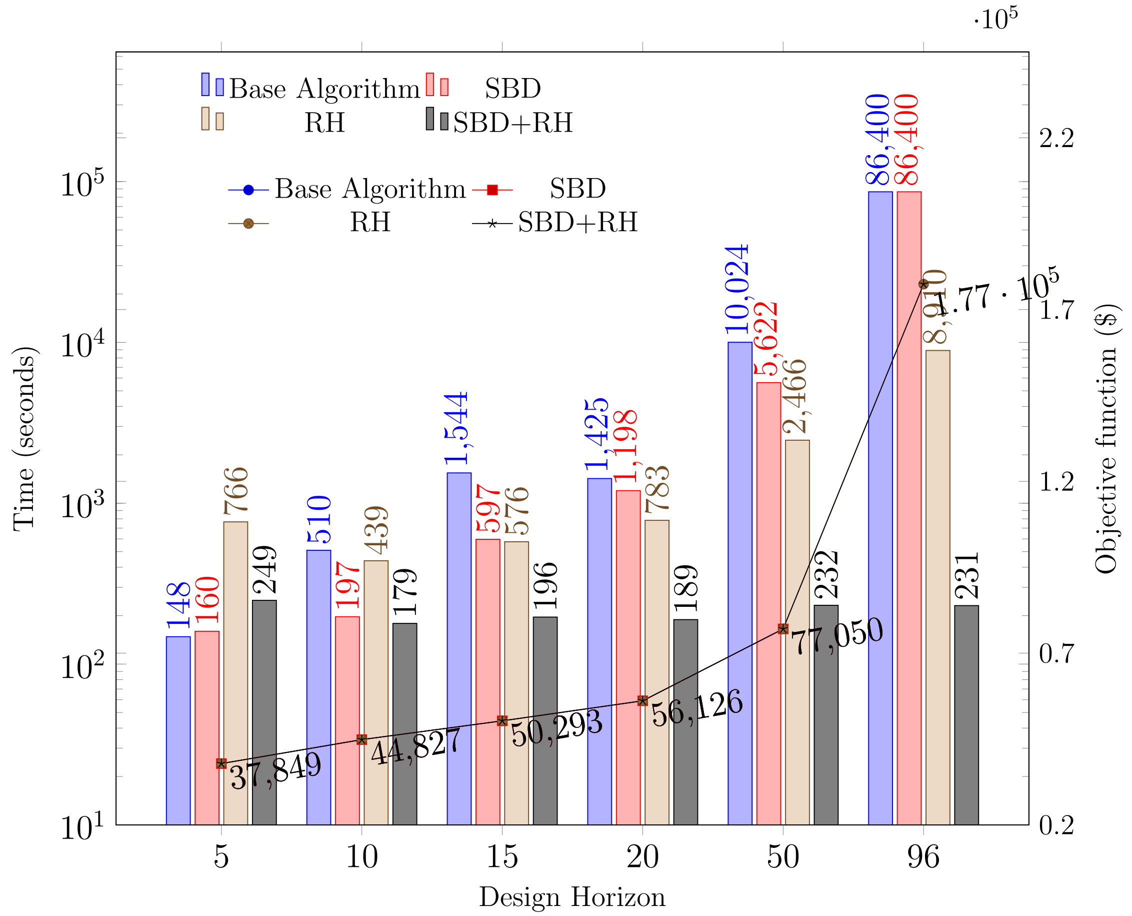

Figure 3.4: Solution times and solution quality for the IEEE 13 case.

RH refers to the rolling horizon algorithm where the base algorithm is used to solve sub problems. SBD+RH refers to the rolling horizon algorithm where SBD is used to solve sub problems. The left y axis shows CPU time (log scale) in seconds. The right y axis shows the objective value. The x axis shows the design horizon ($\mathcal{T}$)

optimal solution for design horizons with less than 50 time-steps. The solutions from the base algorithm were identical to the solutions resulting from other three algorithms for each design horizons. Based on these results, we see that under this model the RH algorithm is generally more computationally efficient than the exact methods and is still able to get solutions of the same quality. However, it is important to stress the RH is a heuristic [23].

3.5.2 Case Study 2: Alaskan Microgrid

In this section, we test the performance of the RH algorithm on an Alaskan micogrid that has 19 nodes and 18 lines (Figure 3.5). In this model a single discrete resource (D_1 through D_5) is allowed to be installed at each node 6, 8 , 10 , 14, and 18 (Table 3.3). Demands for this system are based on data provided by the Alaskan distribution utility. Installation and operational costs are provided in Table 3.3. Table 3.4 describes the specifications of the lines in this system. This network has five existing generators at nodes 1 and another one generator at node 3. All these six existing generators are of type D_1. The capacity of the existing generators is modified so that model is forced to build new generators. Parallel lines may be built anywhere in the system, provided a line currently exists, for a cost of $1000 per line. There are seven generator contingencies and 36 possible line contingencies in the network. The seven generator contingencies are due to five new generators and one existing generator each at node 1 and 3. Altogether, there are 43 contingencies for this network.

TABLE 3.3: Characteristics of technology options for Case Study 2

Tech Type	Fixed Cost ($)	Operational Cost aP^2+bP+c ($)	Rated Power (Max, Min) (KW)
D_1	20000	$50P^2 + 25P + 6$	(200 , 0)
D_2 - D_5	50000	$60P^2 + 20P + 5$	(1500 , 0)

3.5.2.1 Recommended Solution for 96 Design Horizon

The solution for this mirogrid installs generators of type $D2$ at nodes 6, 8, 10, 14 and 18. The solution also installs parallel lines at all locations to support N-1

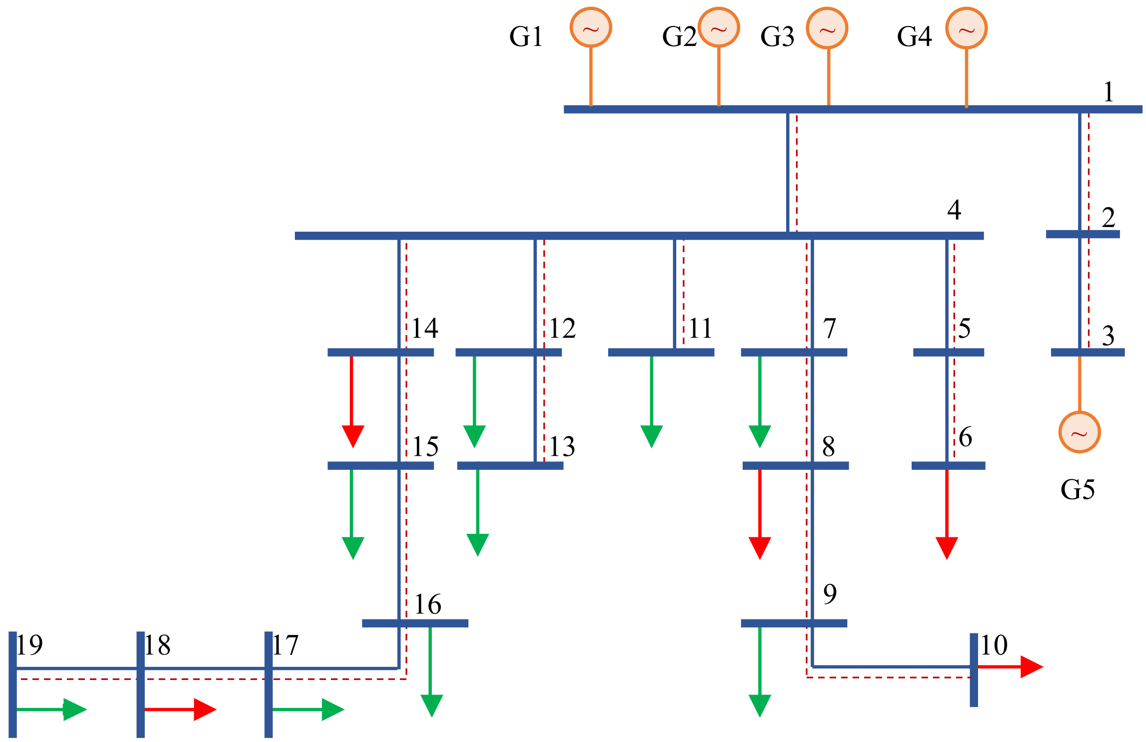

Figure 3.5: Schematic diagram with topology options of a remote community in Alaska

security. This solution changes if they relative cost of adding lines increases.

3.5.2.2 Solution Time

Figure 3.6 compares the solution time for design horizons of 5, 10, 15, 20, and 96. Here, all algorithms had a 24 hour time limit. The two exact methods found the optimal solution only for the case when the time horizon was 5. The proposed rolling horizon algorithm was able to solve this model in 17807 seconds. Interestingly, RH with the base algorithm out performed RH with SBD. On this problem, most of the contingencies must be added to $\mathcal{M}$, a situation that limits the effectiveness of SBD.

TABLE 3.4: Line configuration for Case study 2

ID	Resistance pu	Reactance pu	Thermal Limit MVA	Lines (From node - To node)
A	0	0.05	10000	(1–2), (1–4), (5–6)
B	0.392921923	0.923131194	3422.532396	(2–3)
C	0.157168769	0.369252478	3422.532396	(4–5)
D	0.002854927	0.005210712	3782.798964	(4–7), (7–8)
E	0.019646096	0.04615656	3422.532396	(8–9)
F	0.039292192	0.092313119	3422.532396	(9–10)
G	0.314337539	0.738504956	3422.532396	(4–11), (4–12)
H	0.1021597	0.240014111	3422.532396	(12–13)
I	0.248685034	0.20405299	1585.172899	(4–14)
J	0.373027551	0.306079486	1585.172899	(14–15)
K	0.062171258	0.051013248	1585.172899	(15–16)
L	0.497370068	0.408105981	1585.172899	(16–17), (17–18
M	1.243425169	1.020264952	1585.172899	(18–19)

3.5.3 Sensitivity Analysis

We performed sensitivity analysis on our models by changing the types of generators and the costs for generators and lines. In a hypothetical situation where the installation cost for lines is larger than the installation and operation costs for generators, the model recommended to install generators in each node instead of installing parallel lines. The number of parallel lines installed in those scenarios is less than in the original model. This analysis helps understand the sensitivity of the solutions obtained to changes in problem parameters.

3.6 Conclusion

In this paper, we develop a mathematical formulation for designing and operating remote off-grid microgrids with N-1 security constraints on generators and lines. We also present a rolling horizon algorithm that efficiently solves these problems. There remain a number of interesting future directions for this research.

For example, this model assumes that all generation and demand is deterministic. Future work should consider how to incorporate stochastic renewable resources such as wind and solar. One attractive model is the probabilistic chance constraints used in Sundar *et al.* [89]. Second, methods should be explored to improve the scalability of solving ACIPRM problems in both the size of the networks and the length of the time horizons.

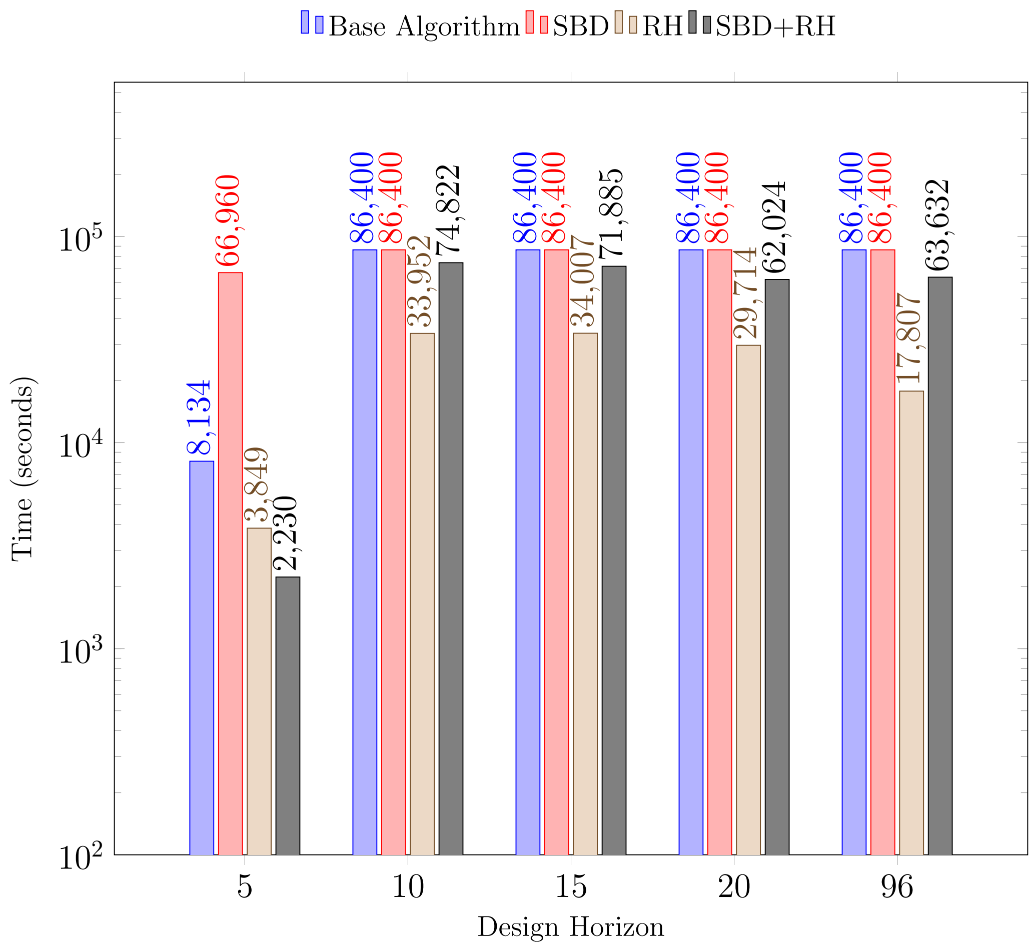

Figure 3.6: Solution times and solution quality for the Alaskan microgrid case.

RH refers to the rolling horizon algorithm where the base algorithm is used to solve sub problems. SBD+RH refers to the rolling horizon algorithm where SBD is used to solve sub problems. The left y axis shows CPU time (log scale) in seconds. The right y axis shows the objective value. The x axis shows the the design horizon ($\mathcal{T}$)

Chapter 4

Design and Operation of Resilient Off-grid Microgrids under Uncertainty

4.1 Introduction

There are many communities in the arctic region that currently rely heavily on diesel generators for their power demands [44]. The use of such fossil fuels in these areas has resulted in a higher cost of power generation due to higher shipping, transportation and storage costs, along with a higher reliance on international fuel supply lines. Moreover, the use of such fuels also result in higher emissions of greenhouse gases (GHG) to the atmosphere [92]. Many remote communities in Alaska like Savoonga and Buckland are some of the first communities in US that have been impacted by the effects of climate change [60]. There are local energy networks, also known as microgrids, that provide power to communities, either in stand-alone mode or in grid-connected mode using distributed energy resources like diesel generators, windmills, solar panels, and hydroelectric generations [71, 91].

There is a strong push to adopt renewable generation in many communities to reduce the environmental and economic concerns due to fossil fuel generators and to reduce the looming threat of global warming [45, 79]. According to the key recommendations in the report of Allen *et al.* [6], a larger role of cost-effective renewable energy can reduce power consumption cost and thereby enhance the self-sufficiency of these rural communities in Alaska. Typically, renewable energy resources include water, sun, wind, geothermal heat, tides and biomass [27]. Of these renewable energy generation technologies, solar and wind energy often are intermittent in nature, implying that there is an inherent uncertainty in power generation when these technologies are used [23, 37].

According to Sciulli [83], a microgrid design support tool should include constraints to account for power generation variability. Chalil Madathil *et al.* [19] provides a deterministic model to design and operate an off-grid microgrid with security constraints as the preliminary research upon which this work is based. One of the main assumptions it serves in Chalil Madathil *et al.* [19] is that power generation is deterministic and there exists no variability in generation or demand. However, in reality, power systems are prone to experience uncertainty, like fluctuations in power generation due to variability inherent in wind and solar energy, demand variability, and unexpected failures within the power network. In this paper, we develop a mathematical model for designing and operating a resilient off-grid microgrid by considering uncertainties in power generation due to solar or wind energy.

The main contributions of this paper are as follows:

- We formulate a mathematical model to design and operate a resilient off-grid microgrid that considers generation uncertainties.

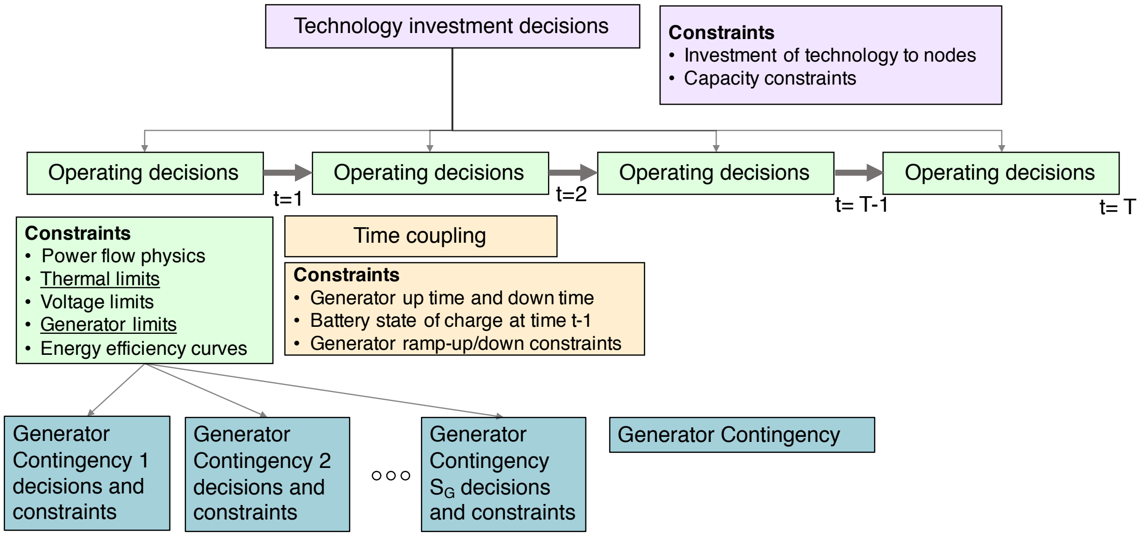

Figure 4.1: Modified flowchart of ACIRPM model with uncertainty [19]

- We develop an efficient algorithm to solve this model in a reasonable amount of time.
- To apply this algorithm on two different network instances and validate our results.

4.1.1 Literature Review

The importance and advantages of renewable energy sources for power generation are discussed in many previous research works [10, 32, 34, 35]. Bajpai *et al.* [10] discusses and reviews various models that use renewable energy resources in combination with either conventional resources like diesel generators or more than one renewable energy source for standalone systems. Such systems are called hybrid renewable energy systems (HRES). Erdnic *et al.* [32] discuss various models that deal with optimum sizing approaches for grid-parallel application modes as well as stand-alone mode for HRES. Fadee and Radzi [34] provide an overview of multi-objective optimization of stand-alone HRES by comparing competing objectives like placement, sizing, design and operation. A practical implementation of a stand-alone HRES is described in [35] that uses hybrid optimization using genetic algorithm to design a HRES with PV, wind and battery. Most of these papers emphasize the need for considering optimization and unit sizing while designing HRES because over-sizing capacity increases overall cost, whereas under-sizing can result in power supply failure. While these studies focus on certain individual aspects of power system design like optimal sizing, unit commitment, optimal power-flow, economic dispatch, reliability, and component efficiencies, we consider all these factors together to make the best decision possible for the system.

The typical causes of uncertainty in power systems include forecasting errors, load fluctuations, generator availability, line outages, and price fluctuations [85, 52, 3]. As stated before, these uncertainties are more prominent when renewable sources like wind and solar are installed in the network. Aien *et al.* [3] provide a comprehensive list of papers that use uncertainty modeling techniques (like stochastic modeling, fuzzy arithmetic, and robust optimization) to study different types of power systems. While designing a system which contains uncertain environment, it is important to consider various issues like (1) can the uncertainty on power generation resources satisfy all the demands? (2) can the capacity of transmission lines withstand this variability when it has to transmit higher current? and (3) can the existing assets absorb these changing trends in generations [22]? Deterministic models can fail to provide insights in making strategic decisions as compared to when we consider these uncertainties. For instance, Siddiqui and Marnay [85] provide an example of loss in investment value resulting from not considering uncertainty in fuel price fluctuations.

There are a lot of research works within the microgrid community that consider uncertainty due to wind and solar [93, 46, 79, 84, 73]. Wang *et al.* [93] devises a two-stage algorithm to minimize electricity generation costs by optimally scheduling demand and supply profiles. The uncertainty of renewable resources are confined to a distribution based on a reference distribution from the past observations or empirical knowledge for the uncertainty. But this model did not consider technology siting, capacity, security constraints, and efficiencies. Hytowitz and Hedman [46] discuss about a two-stage stochastic model for economic dispatch problem incorporating solar uncertainty. The model they developed did not consider modelling of storage, technology siting, capacity, N-1 security and component efficiencies. Shin *et al.* [84] discuss a stochastic model by considering wind uncertainty for optimal sizing and operational planning of hybrid microgrids. They developed a two-stage stochastic model which consists of unit commitment, economic dispatch and technology sizing of microgrids with inherent wind uncertainty. Narayan *et al.* [73] also proposes a two-stage stochastic model for optimizing microgrid planning and operation under uncertainty. They use a copula-based dependence model coupled a Kumaraswamy distribution [55] to model the uncertainty in wind and a separate Kumaraswamy distribution to model stochastic nature of solar energy. Their approach provides reliable, economical and environmentally acceptable solutions. However, no previous research considers technology siting, component efficiencies and N-1 security analysis of the model as we propose. A comparative study from Chalil Madathil *et al.* [19], shows that there can be considerable depletion of solution quality if we ignore all these factors while designing off-grid microgrids.

The design and analysis of microgrids also employ different simulation and meta-heuristic based techniques as discussed in [34, 57, 79]. Fadee and Radzi [34] discusses various approaches using heuristic algorithms like genetic algorithm, and particle swarm optimization and simulation approaches like HOMER, Hybrid2, and HOGA. Rahman *et al.* [79] propose a simulation-based approach using HOMER software [30] for uncertainty modelling due to non-deterministic renewable generation. Kuznetsova *et al.* [57] provide an Agent-Based Model to guide the stakeholder decision options using robust optimization by modelling "extreme" uncertainties in wind power generation and demand utilization. Even though they consider different generation assets, different levels of renewable penetration, and generation uncertainty, these models use simulation-based or heuristic-based methods which may not guarantee even upper or lower bounds for the model.

The chance-constrained model for optimal power flow (OPF) is explained in [14, 96]. One of the major issues while modelling wind uncertainty is to consider the risk of component failures during excessive wind power generation [89]. The authors employ a chance-constrained model and used linear outer approximations, scenario-based decomposition, and Benders Decomposition techniques to their N-1 security and chance-constrained unit commitment (SCCUC) problem. In this model they solve a unit commitment problem with wind uncertainty and N-1 security on generators and lines, but faced computational scalability issues. Sundar *et al.* [90] use a modified Benders decomposition algorithm to solve their SCCUC problem. Our proposed model considers unit commitment, optimal power flow, efficiencies, uncertainties, N-1 security on line and generators for the stand-alone microgrids, which is different than previous efforts.

It is clear from reviewing the literature that considering uncertainty in power generation is important while devising a strategic plan to design and operate an off-grid microgrid. Similarly, there are many models that consider various aspects of microgrid design like technology siting and capacity, unit commitment, OPF, component efficiencies, storage, N-1 security on generators and lines, and generators uncertainty. But none of them considers all these aspects which is the main focus of our paper. We will use chance-constraints method to solve the model in reasonable amount of time.

The rest of the paper is organized as follows. Section 2 deals with model description and explains our stochastic models along with the parameters in the model. We also discuss the modeling of uncertainties in our model. Section 3 describes the algorithm that will be used to solve this model in reasonable amount of time, followed by a demonstration of the algorithm on two case studies in Section 4. We conclude our research findings in Section 5 and provide a brief summary of future research directions.

4.2 Mathematical Formulation

In this section we present the ACIRPM model. The ACIRPM model combines expansion planning decisions with time extended operations, resource planning, efficiencies, and N-1 security criteria to optimize a microgrid for resilience.

4.2.1 Model Parameters and Variables

Sets

$\mathcal{N}$ set of nodes (buses), indexed by i

$\mathcal{E}$ set of existing edges (lines and transformers), indexed by e_{ij}. Each edge is assigned an arbitrary direction from a bus i to a bus j. ij is omitted when direction is not needed.

$\mathcal{E}_n$ set of new edges (lines and transformers), indexed by e_{ij}. Each edge is assigned an arbitrary direction from a bus i to a bus j. ij is omitted when direction is not needed.

$\mathcal{E}_i^+$	set of existing and new edges connected to bus i and oriented from i, indexed by e
$\mathcal{E}_i^-$	set of existing and new edges connected to bus i and oriented to i, indexed by e
$\mathcal{T}$	set of time periods, indexed by t, numbered from 1 to $\|\mathcal{T}\|$
$\mathcal{C}$	set of continuous resources, indexed by c
$\mathcal{C}^D \subseteq \mathcal{C}$	set of continuous resources with discrete operation, indexed by c
$\mathcal{C}^C \subseteq \mathcal{C}$	set of continuous resources with continuous operation, indexed by c
$\mathcal{C}^B \subseteq \mathcal{C}^C$	set of continuous battery resources, indexed by c
$\mathcal{C}^{PV} \subseteq \mathcal{C}^C$	set of continuous PV resources, indexed by c
$\mathcal{C}_i^C \subseteq \mathcal{C}$	set of continuous resources at bus i, indexed by c
$\mathcal{C}_i^{CB} \subseteq \mathcal{C}$	set of continuous resources with storage capabilities at bus i, indexed by c
$\mathcal{D}$	set of discrete resources, indexed by d
$\mathcal{D}^D \subseteq \mathcal{D}$	set of discrete resources with discrete operation, index by d
$\mathcal{D}^C \subseteq \mathcal{D}$	set of discrete resources with continuous operation, indexed by d
$\mathcal{D}^W \subseteq \mathcal{D}$	set of discrete resources that uses wind energy, index by d
$\mathcal{D}_i \subseteq \mathcal{D}$	set of discrete resources at bus i, indexed by d
$\mathcal{A} = \mathcal{C} \cup \mathcal{D}$	set of all resources, indexed by a
$\mathcal{A}_i \subseteq \mathcal{A}$	set of resources at bus i, indexed by a
$\mathcal{A}^C \subseteq \mathcal{A}$	set of control capable resources, indexed by a
$\mathcal{A}^R \subseteq \mathcal{A}$	set of renewable resources, indexed by r

Ω	set of scenarios for N-1 security analysis, indexed by ω

Parameters

f_a	fixed cost for resource $a \in \mathcal{A}$, (\$)
g_a	variable cost for resource $a \in \mathcal{A}$, (\$/MW)
$\kappa_{a,0}, \kappa_{a,1}, \kappa_{a,2}$	fixed, linear, and quadratic operational cost for resource $a \in \mathcal{A}$, (\$)
f_e	installation cost for line $e \in \mathcal{E}_n$, (\$)
$\overline{u}_d$, $\underline{u}_d$	minimum up-time and down-time for resource $d \in \mathcal{D}D$, (time-step)
$\overline{\gamma}_d$, $\underline{\gamma}_d$	ramp up and ramp down rate for resource $d \in \mathcal{D}$, (MW/time-step)
s_e	apparent power thermal limit on line $e \in \mathcal{E}$, (MVA)
lp_i^t, lq_i^t	Active and reactive power demand at bus $i \in \mathcal{N}$ at time $t \in \mathcal{T}$, $(\mathrm{MW}, \mathrm{MVAr})$
$\overline{pg}_a, \overline{qp}_a$	maximum active and reactive power generated by a resource $a \in \mathcal{A}$, $(\mathrm{MW}, \mathrm{MVAr})$
$\underline{pg}_a, \underline{qp}_a$	minimum active and reactive power generated by a resource $a \in \mathcal{A}$, (MW)
Γ_c	maximum energy storage capacity of the battery $c \in \mathcal{C}^B$, (MVA)
$\underline{v_i}, \overline{v_i}$	Squared voltage lower and upper bound at bus $i \in \mathcal{N}$, $((kV)^2)$
$\overline{s}_a$	maximum apparent power generated by resource $a \in \mathcal{A}$, (MVA)
l_a^p	Stand-by loss (y intercept) of a resource $a \in A$ for each piecewise function $p \in \{1, .., P\}$, (MW)
$[\eta_a^1 \dots \eta_a^p]$	Vector of piecewise marginal efficiencies of maximum rated power, (%)
$\mathrm{r}_e, \mathrm{x}_e$	Resistance and reactance of line $e \in \mathcal{E}$, $(k\Omega)$

δt duration of a time-step, (hr)

h_i Maximum number of continuous resources at bus i

k_i Maximum number of discrete resources at bus i, indexed by k_i

π_e Probability of acceptable thermal limit violations

π_p Probability of acceptable active power capacity violations

π_q Probability of acceptable reactive power capacity violations

ς Power ratio for the network

Binary Decision Variables: Discrete technology

x_d^t active/inactive status for resource $d \in \mathcal{D}$ at time $t \in \mathcal{T}$

y_d^t start-up status for resource $d \in \mathcal{D}$ at time $t \in \mathcal{T}$

w_d^t shut-down status for resource $d \in \mathcal{D}$ at time $t \in \mathcal{T}$

b_d status indicator if discrete resource $d \in D$ is built

Binary Decision Variables: Continuous technology

b_c status indicator if continuous resource $c \in C$ is built

Continuous decision variables: Discrete technology

pg_d^t ac active power generation during time $t \in \mathcal{T}$ for discrete resource $d \in \mathcal{D}$, (MW)

qg_d^t ac reactive power generation during time $t \in \mathcal{T}$ for discrete resource $d \in \mathcal{D}$, (MVAr)

$\hat{pg}_d^t$ ac active power generation before losses during time $t \in \mathcal{T}$ for discrete resource $d \in \mathcal{D}$, (MW)

Continuous decision variables: Continuous technology

$\tilde{pg}_c, \tilde{qp}_c$	installed maximum active and reactive power generated by a resource $c \in \mathcal{C}$, (MW, MVAr)
$\tilde{s}_c$	installed maximum apparent power generated by resource $c \in \mathcal{C}$, (MVA)
pg_c^t, qg_c^t	ac apparent power generation during time $t \in \mathcal{T}$ for continuous resource $c \in \mathcal{C}$, (MW, MVAr)
$\hat{pg}_c^t$	ac active power generation before losses during time $t \in \mathcal{T}$ for continuous resource $c \in \mathcal{C}$, (MW)
ς_c^t	Energy stored (state of charge) in the continuous resource battery $c \in \mathcal{C}^B$ at time $t \in \mathcal{T}$, (MW-hr)

Continuous decision variables: Others

$\mathrm{p}_e^t, \mathrm{q}_e^t$	Active and reactive power flow though edge $e \in \mathcal{E}$ at time $t \in \mathcal{T}$, (MW, MVAr)
v_i^t	Squared voltage at node $i \in \mathcal{N}$ at time $t \in T$, $((kV)^2)$
$lp_i^{t,s}, lq_i^{t,\omega}$	apparent power slack at node $i \in \mathcal{N}$ at time $t \in T$ during contingency scenario $\omega \in \Omega$, (MW, MVAr)
ψ_a^t	participation factor for controllable generator $a \in \mathcal{A}^C$ at time-step $t \in \mathcal{T}$

There are both deterministic and random parameters in this model. With this in mind, we denote random variables as **bold** characters for the rest of this chapter in order to enhance readability and understanding. The actual deviation of the power generated ($p\varpi_r^t$ and $q\varpi_r^t$) from the forecast using renewable generation sources is modeled using the random variable $\boldsymbol{\varpi_r^t}$. We calculate the total active power mismatch as $\mathbf{\Delta^t} = \sum_{r\in A^R} \boldsymbol{\varpi_r^t}$. The random variable $\boldsymbol{\varpi_r^t}$causes fluctuations in power dispatch ($\mathbf{\hat{pg}}_a^t$) and line flow ($\mathbf{p}_e^t$) [62, 80]. We also assume that the random variable $\boldsymbol{\varpi_r^t}$is independent and normally distributed with a mean value of zero and known variance σ_r^2. Furthermore, the total power mismatch ($\mathbf{\Delta^t}$) is divided among the set of control-capable generators according to their participation factor ψ_a.

4.2.2 Objective Function

The objective function (4.1a) minimizes the total installation and operation cost of energy resources and enhances network resiliency [19]. The operation costs also contain the expected costs for renewable energy generation.

$$\begin{aligned}
&\min \Big\langle \ \Big(\sum_{i\in\mathcal{N}}\sum_{t\in\mathcal{T}}\sum_{\omega\in\Omega}(|lp_{i,t}^{\omega}| + |lq_{i,t}^{\omega}|)\Big), \\
&\Big(\sum_{c\in\mathcal{C}} f_c b_c + \sum_{c\in\mathcal{C}\setminus\mathcal{C}^B} g_c \tilde{pg}_c + \sum_{c\in\mathcal{C}^B} g_c \tilde{s}_c\Big) + \sum_{d\in\mathcal{D}} f_d b_d + \\
&\mathbb{E}\Big[\sum_{t\in T}\sum_{a\in\mathcal{A}} \big((\kappa_{a,2})(\mathbf{\hat{pg}}_a^t)^2 + (\kappa_{a,1})(\mathbf{\hat{pg}}_a^t) + (\kappa_{a,0})(b_a)\big)\Big] \ \Big\rangle
\end{aligned} \tag{4.1a}$$

4.2.3 Uncertainty Modeling

The uncertainty of wind and solar power generation is modelled using equations (4.2a) and (4.2b). We define $p\varpi_r^t$ and $q\varpi_r^t$ as the known forecast of active and reactive power from renewable sources, respectively, where $\boldsymbol{\varpi_r^t}$is a random variable with known standard deviation [14]. Similarly the reactive power injections are modelled as a factor of the power ratio denoted by the variable ς [80].

$$\mathbf{\hat{pg}_r^t} = p\varpi_r^t + \boldsymbol{\varpi_r^t} \qquad \forall\, i \in \mathcal{N}, r \in \mathcal{A}^R, t \in \mathcal{T} \tag{4.2a}$$

$$\mathbf{\hat{qg}_r^t} = q\varpi_r^t + \varsigma\boldsymbol{\varpi_r^t} \qquad \forall\, i \in \mathcal{N}, r \in \mathcal{A}^R, t \in \mathcal{T} \tag{4.2b}$$

4.2.4 Generator Control

The power generated by wind turbines depends on the velocity of the wind, while the power generated by PV cells depend on solar irradiance [74]. Windmills will either generate or curtail power as long as the wind speed is between certain threshold values. Hence, we look into two scenarios: the case when power generated is less than the forecast value and the case when the power generated is greater than the forecast value. Appropriate constraints should be added to the model in such a way that other controllable generators like diesel and batteries in the network should supplement the necessary demand due to insufficient power generation by wind and/or solar. Similarly, if wind output is increased, then other generators will proportionally decrease. According to Bienstock *et al.* [14], the fluctuation in renewable generation can be modeled as in equation (4.3a), where ψ_a is the participation of controllable generators. Constraints (4.3b) guarantee that the controllable generators respond proportionally to meet the demand.

$$\hat{\mathbf{pg}}_{\mathbf{a}}^{\mathbf{t}} = \hat{pg}_a^t - \psi_a^t \boldsymbol{\Delta}^{\mathbf{t}} \qquad \forall\, a \in \mathcal{A}^C, t \in \mathcal{T} \tag{4.3a}$$

$$\sum_{a \in \mathcal{A}^C} \psi_a^t = 1 \qquad \forall\, t \in \mathcal{T} \tag{4.3b}$$

$$\psi_a^t \leq b_a \qquad \forall\, a \in \mathcal{A}^C, t \in \mathcal{T} \tag{4.3c}$$

4.2.5 Power Flow Physics

The power flow physics in the model includes both Kirchoff's Law and Ohm's Law. Kirchoff's Law is shown in equations (4.4a)-(4.4b), while (4.4c) represents the

LinDistFlow equations of Ohm's Law as described in [36, 12].

$$\sum_{a \in \mathcal{A}_i^C} \mathbf{pg}_a^t + \sum_{r \in \mathcal{A}_i^R} \mathbf{pg}_r^t - lp_i^t = \sum_{e \in \mathcal{E}_i^+} \mathbf{p}_e^t - \sum_{e \in \mathcal{E}_i^-} \mathbf{p}_e^t \qquad \forall\, i \in \mathcal{N}, t \in \mathcal{T} \tag{4.4a}$$

$$\sum_{a \in \mathcal{A}_i^C} \mathbf{qg}_a^t + \sum_{r \in \mathcal{A}_i^R} \mathbf{qg}_r^t - lq_i^t = \sum_{e \in \mathcal{E}_i^+} \mathbf{q}_e^t - \sum_{e \in \mathcal{E}_i^-} \mathbf{q}_e^t \qquad \forall\, i \in \mathcal{N}, t \in \mathcal{T} \tag{4.4b}$$

$$v_j^t = v_i^t - 2(\mathrm{r}_e \mathbf{p}_e^t + \mathrm{x}_e \mathbf{q}_e^t) \qquad \forall\, e_{ij} \in \mathcal{E}, t \in \mathcal{T} \tag{4.4c}$$

4.2.6 Capacity Limits and Operating Status

As previously defined in [19], voltage limits (4.5a), generator ON/OFF status (4.5e)-(4.5g), minimum up-time and down-time (4.5h)-(4.5i), and ramp-up and ramp-down constraints (4.5k)-(4.5k) are required in the model. Similarly, equations (4.5l)-(4.5n) denote the battery operating constraints. The boundary condition for up-time and down-time are defined as $\Upsilon_d = \rho \in \mathcal{T} : t - \overline{u}_d + 1 \leq \rho \leq t$ and $\zeta_d = \rho \in \mathcal{T} : t - \underline{u}_d + 1 \leq \rho \leq t$.

$$\underline{\mathrm{v}_i} \leq v_i^t \leq \overline{\mathrm{v}_i} \qquad \forall\, i \in \mathcal{N}, t \in \mathcal{T} \tag{4.5a}$$

$$\tilde{\mathbf{s}}_c \leq b_c \overline{s}_c \qquad \forall\, c \in \mathcal{C}^B \tag{4.5b}$$

$$\sum_{c \in \mathcal{C}_i} b_c \leq h_i \qquad \forall\, i \in \mathcal{N} \tag{4.5c}$$

$$\sum_{d \in \mathcal{D}_i} b_d \leq k_i \qquad \forall\, i \in \mathcal{N} \tag{4.5d}$$

$$x_d^t \leq b_d \qquad \forall\, d \in \mathcal{D}^D, t \in \mathcal{T} \tag{4.5e}$$

$$x_d^t = x_d^{t-1} + y_d^t - w_d^t \qquad \forall\, d \in \mathcal{D}^D, t \in \mathcal{T} \tag{4.5f}$$

$$y_d^t + w_d^t \leq 1 \qquad \forall\, d \in \mathcal{D}^D, t \in \mathcal{T} \tag{4.5g}$$

$$\sum_{\rho \in \Upsilon_d} y_d^\rho \leq x_d^t \qquad \forall\, d \in \mathcal{D}^D, t \in \mathcal{T} \tag{4.5h}$$

$$\sum_{\rho \in \zeta_d} w_d^{\rho} \leq 1 - x_d^t \qquad \forall\ d \in \mathcal{D}^D, t \in \mathcal{T} \tag{4.5i}$$

$$\overline{\gamma}_d \geq \mathbf{pg}_d^t - \mathbf{pg}_d^{t-1} - \overline{pg}_d y_d^t \qquad \forall\ d \in \mathcal{D}^D t \in \mathcal{T} \tag{4.5j}$$

$$\underline{\gamma}_d \geq \mathbf{pg}_d^{t-1} - \mathbf{pg}_d^t - \overline{pg}_d w_d^t \qquad \forall\ d \in \mathcal{D}^D t \in \mathcal{T} \tag{4.5k}$$

$$(\mathbf{pg}_c^t)^2 + (\mathbf{qg}_c^t)^2 \leq (\tilde{\mathbf{s}}_c)^2 \qquad \forall\ c \in \mathcal{C}^B, t \in \mathcal{T} \tag{4.5l}$$

$$\mathfrak{e}_c^t = \mathfrak{e}_c^{t-1} - \hat{\mathbf{pg}}_c^t \delta t \qquad \forall\ c \in \mathcal{C}^B, t \in \mathcal{T} \tag{4.5m}$$

$$0 \leq \mathbf{s}_c^t \leq \tilde{\mathbf{s}}_c \qquad \forall\ c \in \mathcal{C}^B, t \in T \tag{4.5n}$$

4.3 Need for Stochasticity

All numerical experiments were performed using a Microsoft Windows® Server 2016 running an Intel® Core™ i7-6950X CPU @ 3.00 GHz processor with 10 cores and 128 GB RAM. The model was implemented using JuMP modeling software [28] and Gurobi V7.0.1 solver [41].

4.3.1 Problem Setup

In order to test our model, we create a toy three-node model (Figure 4.2) using the IEEE 13 node test case [50]. Node 632 can install a storage device, whereas node 645 has a diesel generator. Node 646 has a windmill which has example values of predicted forecast for active and reactive power output. Variations in this forecast introduces randomness in our model. The maximum power that can be generated by windmill is $15kW$ per time-step. The demand at each node, wind forecast at node 646, and forecast errors for two samples are shown in Table 4.2. The two samples show borderline cases of wind generation. Sample 1 provides random power generation that is mostly less than net demand whereas sample 2 provides random power generation that is always greater than net demand. We adopt other network parameters such as line limits, resistance, and reactance from Chalil Madathil *et al.* [19].

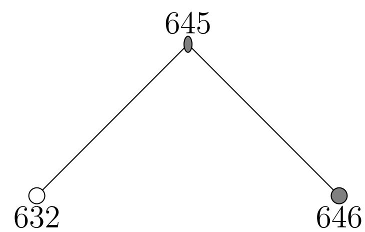

Figure 4.2: A test three node network

TABLE 4.2: Demand and wind generation profile

Time period	Node name	Demand Active (kW)	Demand Reactive (kVA)	Wind forecast Active (kW)	Wind forecast Reactive (kVA)	Forecast Error Sample 1	Forecast Error Sample 2
1	632	0.240	0.149	-	-	-	-
	645	0.631	0.391	-	-	-	-
	646	0.039	0.024	2.1	2.1	-0.329068	0.407678
2	632	1.432	0.887	-	-	-	-
	645	0.614	0.381	-	-	-	-
	646	0.037	0.023	1.9	1.9	0.191877	1.34538
3	632	2.196	1.361	-	-	-	-
	645	0.556	0.345	-	-	-	-
	646	0.080	0.050	1.4	1.4	-0.30071	0.458721
4	632	0.266	0.165	-	-	-	-
	645	0.560	0.347	-	-	-	-
	646	0.139	0.086	1.3	1.3	-0.105758	0.809635
5	632	0.266	0.165	-	-	-	-
	645	0.554	0.343	-	-	-	-
	646	0.131	0.081	1.4	1.4	0.78937	2.42087

4.3.2 Example Cases

In order to study the importance of incorporating stochasticity to design and operate off-grid microgrids, we compare scenario results between the deterministic and stochastic model (Table 4.3). While scenarios 1 and 2 are both deterministic

TABLE 4.3: Need for stochasticity

S No	Model type DM/SM	Install options CG	RG	Storage	Model Results CG	RG	Storage	Objective function ($)	Error forecast
1	DM	✓	×	✓	✓	×	×	$21052.50	N/A
2	DM	✓	✓	✓	×	✓	×	$10000.00	N/A
3	SM	✓	✓	✓	✓	✓	✓	$30670.74	Sample 1
4	SM	✓	✓	✓	×	✓	✓	$10545.07	Sample 2

DM - Deterministic Model CG - Conventional Generators
SM - Stochastic Model RG - Renewable Generators

models, the latter uses renewable generators under the assumption of deterministic power generation. We also assume that the operating costs for such renewable sources are zero. Scenarios 3 and 4 have similar generator options, but differ in the samples of forecast error used (Table 4.2) to model stochasticity. When the two samples are run independently, we see two different solutions. For sample 1, which is created to represent a case where random power generation can be less than demand, the model recommends to install a storage device and a diesel generator. Alternatively, the results for sample 2, which has random power generation that is always greater than demand, the model recommends to build a storage device. The storage device is necessary to account for excessive power generation by the windmill rather than for total demand in the network. The model instance is infeasible when we consider a scenario with no option to install any storage device.

While the deterministic model suggests to install only one control capable generator, the stochastic model suggests to install storage and/or auxiliary generator to satisfy the demand and also to address the variability. Even though the objective value of deterministic model is lower than the stochastic model in this test instance, a larger time horizon problem instance will most likely have higher operating costs for control capable generators due to their quadratic operating costs. Clearly, considering a stochastic model provides a better understanding of the system and suggests to install necessary components in the network.

4.4 Algorithms

4.4.1 Chance Constraints

Equations (4.6a) through (4.6i) are modeled as chance constraints with the values of π being defined by the designer for acceptable violation probabilities. For example, constraint set (4.6a) denote the occurrence of a thermal limit overload.

$$\mathbb{P}\bigg((\mathbf{p}_e^t)^2 + (\mathbf{q}_e^t)^2 \leq (s_e)^2 \bigg) \geq 1 - \pi_e \qquad \forall\, e \in \mathcal{E}, t \in \mathcal{T} \tag{4.6a}$$

$$\mathbb{P}\bigg(\hat{\mathbf{pg}}_c \leq \tilde{pg}_c \bigg) \geq 1 - \pi_p \qquad \forall\, c \in \mathcal{C} \setminus \mathcal{C}^B, t \in \mathcal{T} \tag{4.6b}$$

$$\mathbb{P}\bigg(\hat{\mathbf{pg}}_c \geq b_c \underline{pg}_c \bigg) \geq 1 - \pi_p \qquad \forall\, c \in \mathcal{C} \setminus \mathcal{C}^B, t \in \mathcal{T} \tag{4.6c}$$

$$\mathbb{P}\bigg(\hat{\mathbf{qg}}_c \leq \tilde{qg}_c \bigg) \geq 1 - \pi_q \qquad \forall\, c \in \mathcal{C} \setminus \mathcal{C}^B, t \in \mathcal{T} \tag{4.6d}$$

$$\mathbb{P}\bigg(\hat{\mathbf{qg}}_c \geq b_c \underline{qg}_c \bigg) \geq 1 - \pi_q \qquad \forall\, c \in \mathcal{C} \setminus \mathcal{C}^B, t \in \mathcal{T} \tag{4.6e}$$

$$\mathbb{P}\bigg(\hat{\mathbf{pg}}_d^t \leq \overline{pg}_d x_d^t \bigg) \geq 1 - \pi_p \qquad \forall\, d \in \mathcal{D}^D, t \in \mathcal{T} \tag{4.6f}$$

$$\mathbb{P}\bigg(\hat{\mathbf{pg}}_d^t \geq \underline{pg}_d x_d^t \bigg) \geq 1 - \pi_p \qquad \forall\, d \in \mathcal{D}^D, t \in \mathcal{T} \tag{4.6g}$$

$$\mathbb{P}\bigg(\hat{\mathbf{qg}}_d^t \leq \overline{qg}_d x_d^t \bigg) \geq 1 - \pi_q \qquad \forall\, d \in \mathcal{D}^D, t \in \mathcal{T} \tag{4.6h}$$

$$\mathbb{P}\bigg(\hat{\mathbf{qg}}_d^t \geq \underline{qg}_d x_d^t \bigg) \geq 1 - \pi_q \qquad \forall\, d \in \mathcal{D}^D, t \in \mathcal{T} \tag{4.6i}$$

The chance constraints (4.6a) can be reformulated using two absolute value constraints as in (4.7a) - (4.7c) [61]. Here, $\beta \in (0, 1)$ is a trade-off parameter to measure the violation between equations (4.7a) and (4.7b).

$$\mathbb{P}\bigg(|\mathbf{p}_e^t| \le p_e^t\bigg) \ge 1 - \beta\pi_e \qquad \forall\, e \in \mathcal{E}, t \in \mathcal{T} \tag{4.7a}$$

$$\mathbb{P}\bigg(|\mathbf{q}_e^t| \le q_e^t\bigg) \ge 1 - (1-\beta)\pi_e \qquad \forall\, e \in \mathcal{E}, t \in \mathcal{T} \tag{4.7b}$$

$$(p_e^t)^2 + (q_e^t)^2 \le (s_e)^2 \qquad \forall\, e \in \mathcal{E}, t \in \mathcal{T} \tag{4.7c}$$

4.4.2 Component Efficiencies

Piece-wise linear functions (p) for component efficiences as defined in Chalil Madathil *et al.* [19] are restated in constraints (4.8a) - (4.8c).

$$\mathbf{pg}_c^t \le \eta_c^p \hat{\mathbf{pg}}_c^t + b_c l_c^p \qquad \forall\, c \in \mathcal{C}, t \in \mathcal{T}, p \tag{4.8a}$$

$$\mathbf{pg}_d^t \le \eta_d^p \hat{\mathbf{pg}}_d^t + x_d^t l_d^p \qquad \forall\, d \in \mathcal{D}^C, t \in \mathcal{T}, p \tag{4.8b}$$

$$\mathbf{pg}_d^t \le \eta_d^p \hat{\mathbf{pg}}_d^t + b_d l_d^p \qquad \forall\, d \in \mathcal{D}^D, t \in \mathcal{T}, p \tag{4.8c}$$

4.4.3 Deterministic Equivalent of Chance Constraints

The quadratic cost function in (4.1a) can be rewritten as provided in [62]. The updated objective function is stated in (4.9a).

$$\begin{aligned}
\min \bigg\langle \ & \bigg(\sum_{i\in\mathcal{N}}\sum_{t\in\mathcal{T}}\sum_{\omega\in\Omega}(|lp_{i,t}^{\omega}| + |lq_{i,t}^{\omega}|)\bigg), \\
& \bigg(\sum_{c\in\mathcal{C}} f_c b_c + \sum_{c\in\mathcal{C}\setminus\mathcal{C}^B} g_c \tilde{pg}_c + \sum_{c\in\mathcal{C}^B} g_c \tilde{s}_c\bigg) + \sum_{d\in\mathcal{D}} f_d b_d + \\
& \sum_{t\in T}\sum_{a\in\mathcal{A}}\bigg((\kappa_{a,2})\big[(\hat{pg}_a^t)^2 + \mathrm{var}(\mathbf{\Delta}^t)(\psi_a^t)^2\big] + (\kappa_{a,1})(\hat{pg}_a^t) + (\kappa_{a,0})(b_a)\bigg) \ \bigg\rangle
\end{aligned} \tag{4.9a}$$

We use the method of Urli and Nadeau described by Abdelaziz [2] to define both violation variables (variables $U1$ to $U9$) and slack variables (variables $V1$ - $V9$) for all chance constraints in the model. We present the deterministic form of the chance constraints in (4.10a) through (4.10h) that are applicable for all scenarios $n \in \mho$. They also introduce a new objective function that minimizes the sum of violation variable of the chance constraints $\frac{1}{|\mho|}\sum_{n\in\mho} \varkappa_1 U1 + .. + \varkappa_9 U9$, where $\varkappa$ is the weighted penalty.

$$\hat{\mathbf{pg}}_c^n - \tilde{pg}_c + \mathrm{U2}_c^n - \mathrm{V2}_c^n = 0 \qquad \forall\, c \in \mathcal{C} \setminus \mathcal{C}^B, t \in \mathcal{T} \tag{4.10a}$$

$$\hat{\mathbf{pg}}_c^n - b_c \underline{pg}_c - \mathrm{U3}_c^n + \mathrm{V3}_c^n = 0 \qquad \forall\, c \in \mathcal{C} \setminus \mathcal{C}^B, t \in \mathcal{T} \tag{4.10b}$$

$$\hat{\mathbf{qg}}_c^n - \tilde{qg}_c + \mathrm{U4}_c^n - \mathrm{V4}_c^n = 0 \qquad \forall\, c \in \mathcal{C} \setminus \mathcal{C}^B, t \in \mathcal{T} \tag{4.10c}$$

$$\hat{\mathbf{qg}}_c^n - b_c \underline{qg}_c - \mathrm{U5}_c^n + \mathrm{V5}_c^n = 0 \qquad \forall\, c \in \mathcal{C} \setminus \mathcal{C}^B, t \in \mathcal{T} \tag{4.10d}$$

$$\hat{\mathbf{pg}}_d^{t,n} - \overline{pg}_d x_d^t + \mathrm{U6}_d^n - \mathrm{V6}_d^n = 0 \qquad \forall\, d \in \mathcal{D}^D, t \in \mathcal{T} \tag{4.10e}$$

$$\hat{\mathbf{pg}}_d^{t,n} - \underline{pg}_d x_d^t - \mathrm{U7}_d^n + \mathrm{V7}_d^n = 0 \qquad \forall\, d \in \mathcal{D}^D, t \in \mathcal{T} \tag{4.10f}$$

$$\hat{\mathbf{qg}}_d^{t,n} - \overline{qg}_d x_d^t + \mathrm{U8}_d^n - \mathrm{V8}_d^n = 0 \qquad \forall\, d \in \mathcal{D}^D, t \in \mathcal{T} \tag{4.10g}$$

$$\hat{\mathbf{qg}}_d^{t,n} - \underline{qg}_d x_d^t - \mathrm{U9}_d^n + \mathrm{V9}_d^n = 0 \qquad \forall\, d \in \mathcal{D}^D, t \in \mathcal{T} \tag{4.10h}$$

4.5 Conclusion

In this paper, we develop a mathematical formulation for designing and operating remote off-grid microgrids under uncertain power generation. We also conduct an initial study to understand the need for considering stochasticity in power generation. Further study is required to identify more accurate behavior of our model. Future work should consider N-1 security, large time horizon, and efficient algorithm to solve the model in reasonable amount of time. We should also test our model on standard networks and compare results with real microgrids in terms of solving time.

Chapter 5

Conclusion

Off-grid microgrids provide electricity to remote locations that cannot be connected to the regular power grids. The two major challenges for the design and operation of such off-grid microgrids include system reliability and environmental issues. In this dissertation, we aim to address these two issues in three stages.

5.1 Summary

In the first stage of this dissertation, we develop a mathematical model to help decision makers optimally design and operate an off-grid microgrid by considering N-1 system security. Our model also considers characteristics like the type of generators to be installed, location for generator installation, and their maximum capacities. The operational characteristics contained in our model include dispatch over multiple periods, component efficiencies, physical limits of the network, and power-flow physics. The network design problem combined with nonlinear power flow physics and multiple time periods is a complex problem to solve. Hence, we first consider only generator contingencies. We developed a computationally efficient, scenario-based decomposition (SBD) algorithm to solve the model in a reasonable amount of time. The solutions resulting from the model provide insights on possible solution options such as installing backup generators and/or appropriate power dispatch by the generating units over time.

We expand the ac integrated resource planning problem for microgrids (ACRIPM) to include network topology and N-1 security on transmission lines as well. Our solutions for this expanded model now also include network topology decisions to build new lines and/or redundant lines in addition to the decisions developed in the first stage. Unfortunately, the SBD algorithm failed to solve large problem instances when we include topology decisions. Therefore, we develop a rolling horizon (RH) procedure and a hybrid algorithm that uses the benefits of both SBD and RH to solve our model in an acceptable period of time. The solutions recommend building redundant lines when there is a possibility of islanding of nodes from generating sources, which helps to improve network reliability.

In the first two stages, we focused our model development based on the assumption that power generation is deterministic. In fact, some of the communities that install off-grid microgrids are now increasing the use of renewable energy sources for generation in their networks. With this in mind, we expand our ACRIPM model to include generation uncertainty in stage three. We conducted some initial tests to justify the need for considering stochasticity in designing and operating off-grid microgrids. We propose a chance-constrained optimization technique to address issues related to uncertainties such as exceeding generation capacity of controllable generation and line breakage due to excessive power flow due to renewable generation. The preliminary results recommended to install storage devices to store excess power generated by the renewable resources.

5.2 Future Work

There are multiple directions that we can pursue in the future to enhance this research study. First our models need to be tested on a larger set of microgrid networks at different locations to ensure the quality of solutions recommended by our algorithms are maintained and scale across different locations. With the implementation of stage 3, we considered the ACRIMP model with power generation uncertainties. Further analyses are required to understand the impact of stochasticity on N-1 security analysis. In reality, there also will be demand uncertainty that should be considered in the model. Hence, the current model should be expanded to include demand fluctuations in the network.

The problems that we considered in all three stages of this dissertation consist of only one day's worth of data. We should make optimal strategic decision to build and operate off-grid microgrid by considering the actual life cycle of a microgrid, which is typically 20 years. However, solving such larger horizon problem can be computationally challenging. Hence there exists a need to find smarter ways to incorporate future demands and other systems requirements to obtain accurate results over a longer time horizon.

5.3 Concluding Remarks

During the course of this research, we substantiated the need for considering nonlinear ac power-flows, N-1 security, component efficiencies, time-dependent operations, and stochastic nature of renewable resources in order to design cost-effective and resilient off-grid microgrids. We also developed efficient algorithms to solve this complex model in reasonable amount of time. From the results, we observed that, in order to enhance resilience of certain networks it may not be necessary to install backup generators but installing redundant lines and dispatching power efficiently can also achieve the same objective at reduced cost. This concludes a large part of our research in designing off-grid microgrids with N-1 security analysis and their efficient time-dependent operations.

This dissertation work can also help communities worldwide who have no access to electricity. According to the International Centre for Trade and Sustainable Development (ICTSD), there are over 645 million people in Africa who are still living in darkness with a substantially low quality of life [47]. The potential exists to enhance the quality of life and economic growth for these under-developed communities by installing off-grid microgrids using the methods discussed in this dissertation. In turn, we can strive towards making this world a better place to live.

Appendices

Appendix A License for images

GILDEMEISTER
energy solutions

GILDEMEISTER energy solutions GmbH
Carl-Zeiss-Str. 4
D-97076 Würzburg

GILDEMEISTER energy solutions
T +49 (0) 931 250 64-0
F +49 (0) 931 250 64-104
energysolutions@gildemeister.com
www.gildemeister.com

GILDEMEISTER energy solutions GmbH,
Carl-Zeiss-Str. 4
D-97076 Würzburg, Germany

01.04.2016

Limited grant of use

GILDEMEISTER energy solutions GmbH
Carl-Zeiss-Str. 4
97076 Würzburg
- hereinafter „GILDEMEISTER energy solutions“ -

grants

Sreenath Chalil Madathil
PhD Candidate |129 Freeman Hall
Department of Industrial Engineering
Clemson University SC-29634
- hereinafter the "Authorized" -

a simple and a limited right of use with respect to the ("Works") listed in Appendix A of this agreement which are protected by copyright. The right of use is granted on the following conditions. GILDEMEISTER energy solutions as the copyright owner allows the holder to use the attached work. The claimant has the exploitation rights according to Copyright Act § § 16-22 to use the work for his dissertation.

The right of use is granted without fees payable.

GILDEMEISTER energy solutions has the right to terminate this agreement at any time without notice for any reason.
Law applicable to this agreement is German law. Jurisdiction applied is Würzburg.

GILDEMEISTER energy solutions GmbH	GILDEMEISTER energy solutions GmbH	
Julian Seume Head of Marketing	Vera Gieseke Marketing	Sreenath Chalil Madathil PhD Candidate
.... Name	.... Name	.... Name
01.04.2016 .... Signature Date	01.04.2016 .... Signature Date	April 01, 2016 .... Signature Date

Amtsgericht Würzburg
HRB 4356
Sitz der Gesellschaft: Würzburg
USt-Id.Nr. DE134166879

Geschäftsführung:
Dipl.-Volksw. Dr. Frank Beermann
B.A./MBA André Kremer

Hypovereinsbank
Kto.-Nr.: 326259330
BLZ: 790 200 76
IBAN: DE24 7902 0076 0326 2593 30
SWIFT: HYVEDEMM455

Deutsche Bank
Kto.-Nr.: 066072000
BLZ: 480 700 20
IBAN: DE67 4807 0020 0066 0720 00
BIC: DEUTDE3BXXX

GILDEMEISTER
energy solutions

APPENDIX A:
(will be provided as pdf document or via server upload)

–

–

–

Bibliography

[1] Abb central inverters pvi-500.0-cn 500 kw, 5 2014. Rev. A EN.

[2] Fouad Ben Abdelaziz. Solution approaches for the multiobjective stochastic programming. *European Journal of Operational Research*, 216(1):1–16, 2012.

[3] Morteza Aien, Ali Hajebrahimi, and Mahmud Fotuhi-Firuzabad. A comprehensive review on uncertainty modeling techniques in power system studies. *Renewable and Sustainable Energy Reviews*, 57:1077–1089, 2016.

[4] Réka Albert, István Albert, and Gary L Nakarado. Structural vulnerability of the north american power grid. *Physical review E*, 69(2):025103, 2004.

[5] N Alguacil and AJ Conejo. Multiperiod optimal power flow using benders decomposition. *IEEE Transactions on power systems*, 15(1):196–201, 2000.

[6] Riley Allen, Donna Brutkoski, David Farnsworth, and Peter Larsen. Sustainable energy solutions for rural alaska. Technical report, Lawrence Berkeley National Laboratory (LBNL), Berkeley, CA (United States), 2016.

[7] S Bahramara, M Parsa Moghaddam, and MR Haghifam. Optimal planning of hybrid renewable energy systems using homer: A review. *Renewable and Sustainable Energy Reviews*, 62:609–620, 2016.

[8] Shaghayegh Bahramirad, Wanda Reder, and Amin Khodaei. Reliability-constrained optimal sizing of energy storage system in a microgrid. *IEEE Transactions on Smart Grid*, 3(4):2056–2062, 2012.

[9] Owen Bailey, Charles Creighton, Ryan Firestone, Chris Marnay, and Michael Stadler. Distributed energy resources in practice: A case study analysis and validation of LBNL's customer adoption model. *Lawrence Berkeley National Laboratory*, 2003.

[10] Prabodh Bajpai and Vaishalee Dash. Hybrid renewable energy systems for power generation in stand-alone applications: a review. *Renewable and Sustainable Energy Reviews*, 16(5):2926–2939, 2012.

[11] Bjorn H Bakken, Hans I Skjelbred, and Ove Wolfgang. etransport: Investment planning in energy supply systems with multiple energy carriers. *Energy*, 32(9):1676–1689, 2007.

[12] Mesut E Baran and Felix F Wu. Network reconfiguration in distribution systems for loss reduction and load balancing. *Power Delivery, IEEE Transactions on*, 4(2):1401–1407, 1989.

[13] Zhaohong Bie, Peng Zhang, Gengfeng Li, Bowen Hua, Matthew Meehan, and Xifan Wang. Reliability evaluation of active distribution systems including microgrids. *IEEE Transactions on Power Systems*, 27(4):2342–2350, 2012.

[14] Daniel Bienstock, Michael Chertkov, and Sean Harnett. Chance-constrained optimal power flow: Risk-aware network control under uncertainty. *SIAM Review*, 56(3):461–495, 2014.

[15] Roy Billinton and Ronald N Allan. Power-system reliability in perspective. *Electronics and Power*, 30(3):231–236, 1984.

[16] Aldo Bischi, Leonardo Taccari, Emanuele Martelli, Edoardo Amaldi, Giampaolo Manzolini, Paolo Silva, Stefano Campanari, and Ennio Macchi. A detailed milp optimization model for combined cooling, heat and power system operation planning. *Energy*, 74:12–26, 2014.

[17] Gonçalo Cardoso, Nicholas DeForest, L. Le Gall, Christoph Gehbauer, Michael Hartner, Salman Mashayekh, Christian Milan, Tim Schittekatte, Michael Stadler, David Steen, and Jonas Tjaeder. DER-CAM user manual full DER web optimization service. Technical report, Lawrence Berkeley National Laboratory (LBNL), 1 Cyclotron Rd, Berkeley, CA 94720, 2015.

[18] Caterpillar generator data, 2 2016. 41205 /40476 /41431 /8427.

[19] Sreenath Chalil Madathil, Emre Yamangil, Harsha Nagarajan, Arthur Barnes, Russell Bent, Scott Backhaus, Scott J Mason, Salman Mashayekh, and Michael Stadler. Resilient off-grid microgrids: Capacity planning and n-1 security. *IEEE Transactions on Smart Grid*, 2017.

[20] Liang Che, Xiaping Zhang, Mohammad Shahidehpour, Ahmed Alabdulwahab, and Yusuf Al-Turki. Optimal planning of loop-based microgrid topology. *IEEE Transactions on Smart Grid*, 2016.

[21] Richard Li-Yang Chen and Cynthia A Phillips. k-edge failure resilient network design. *Electronic Notes in Discrete Mathematics*, 41:375–382, 2013.

[22] Lifei Cheng, Eswaran Subrahmanian, and AW Westerberg. Design and planning under uncertainty: issues on problem formulation and solution. *Computers & Chemical Engineering*, 27(6):781–801, 2003.

[23] Javier Silvente, Georgios M Kopanos, Efstratios N Pistikopoulos, and Antonio Espuña. a rolling horizon optimization framework for the simultaneous energy supply and demand planning in microgrids. *Applied Energy*, 155:485–501, 2015.

[24] Alaska Electric Light & Power Company. Outages: Watt's the story. `http://www.aelp.com/outages/outages.htm`.

[25] Paolo Crucitti, Vito Latora, and Massimo Marchiori. A topological analysis of the italian electric power grid. *Physica A: Statistical mechanics and its applications*, 338(1):92–97, 2004.

[26] AW Czanderna, GJ Jorgensen, C Edwin Witt, Mowafak Al-Jassim, and James M Gee. Service lifetime prediction for encapsulated photovoltaic cells/minimodules. In *AIP Conference Proceedings*, volume 394, pages 295–312. AIP, 1997.

[27] Dieter Deublein and Angelika Steinhauser. *Biogas from waste and renewable resources: an introduction*. John Wiley & Sons, 2011.

[28] Iain Dunning, Joey Huchette, and Miles Lubin. Jump: A modeling language for mathematical optimization. *SIAM Review*, 59(2):295–320, 2017.

[29] Chugach Electric. Current power outages. `https://www.chugachelectric.com/customer-service/current-power-outages`, February 2016.

[30] Homer Energy. Energy modeling software for hybrid renewable energy systems. *Overview [online], available: http://homerenergy. com/[accessed 2 nd April 2012]*, 2012.

[31] The Electric Power Research Institute (EPRI). Electric power system resiliency: Challenges and opportunities. Technical Report 3002007376, The Electric Power Research Institute (EPRI), 3420 Hillview Avenue, Palo Alto, California 94304-1338, Feb 2016.

[32] O Erdinc and M Uzunoglu. Optimum design of hybrid renewable energy systems: Overview of different approaches. *Renewable and Sustainable Energy Reviews*, 16(3):1412–1425, 2012.

[33] Melike Erol-Kantarci, Burak Kantarci, and Hussein T Mouftah. Reliable overlay topology design for the smart microgrid network. *IEEE Network*, 25(5), 2011.

[34] M Fadaee and MAM Radzi. Multi-objective optimization of a stand-alone hybrid renewable energy system by using evolutionary algorithms: a review. *Renewable and Sustainable Energy Reviews*, 16(5):3364–3369, 2012.

[35] M Fadaeenejad, MAM Radzi, MZA AbKadir, and H Hizam. Assessment of hybrid renewable power sources for rural electrification in malaysia. *Renewable and Sustainable Energy Reviews*, 30:299–305, 2014.

[36] Lingwen Gan, Na Li, Ufuk Topcu, and Steven H Low. Exact convex relaxation of optimal power flow in radial networks. *Automatic Control, IEEE Transactions on*, 60(1):72–87, 2015.

[37] Robin Girard, K Laquaine, and Georges Kariniotakis. Assessment of wind power predictability as a decision factor in the investment phase of wind farms. *Applied Energy*, 101:609–617, 2013.

[38] Ajit Gopalakrishnan, Arvind U Raghunathan, Daniel Nikovski, and Lorenz T Biegler. Global optimization of optimal power flow using a branch & bound algorithm. In *Communication, Control, and Computing (Allerton), 2012 50th Annual Allerton Conference on*, pages 609–616. IEEE, 2012.

[39] Ajit Gopalakrishnan, Arvind U Raghunathan, Daniel Nikovski, and Lorenz T Biegler. Global optimization of multi-period optimal power flow. In *American Control Conference (ACC), 2013*, pages 1157–1164. IEEE, 2013.

[40] David L Greene. Measuring energy security: Can the united states achieve oil independence? *Energy policy*, 38(4):1614–1621, 2010.

[41] Inc. Gurobi Optimization. Gurobi optimizer reference manual, 2015.

[42] Omar Hafez and Kankar Bhattacharya. Optimal planning and design of a renewable energy based supply system for microgrids. *Renewable Energy*, 45:7–15, 2012.

[43] Yasuhiro Hayashi and Junya Matsuki. Loss minimum configuration of distribution system considering n-1 security of dispersed generators. *IEEE Transactions on power systems*, 19(1):636–642, 2004.

[44] Hannah Hoag. Getting renewable energy into remote communities, Apr 2016.

[45] Enrico Howe, Philipp Blechinger, Catherina Cader, and Christian Breyer. Analyzing drivers and barriers for renewable energy integration to small islands power generation–tapping a huge market potential for mini-grids. In *Micro Perspectives for Decentralized Energy Supply: Proceedings of the International Conference Technische Universität Berlin*, 2013.

[46] Robin Broder Hytowitz and Kory W Hedman. Managing solar uncertainty in microgrid systems with stochastic unit commitment. *Electric Power Systems Research*, 119:111–118, 2015.

[47] "Ambitious plans to electrify africa launched in davos", Jan 2016.

[48] Onur Kahveci, Thomas J Overbye, Nathan H Putnam, and Ahmet Soylemezoglu. Optimization framework for topology design challenges in tactical smart microgrid planning. In *Power and Energy Conference at Illinois (PECI), 2016 IEEE*, pages 1–7. IEEE, 2016.

[49] Ruud Kempener, Olivier Lavagne d'Ortigue, Deger Saygin, Je rey Skeer, Salvatore Vinci, and Dolf Gielen (IRENA). Off-grid renewable energy systems: Status and methodolgical issues. In *Off-grid renewable energy systems*. International Renewable Energy Agency (IRENA), 2015.

[50] William H Kersting. Radial distribution test feeders. In *Power Engineering Society Winter Meeting, 2001. IEEE*, volume 2, pages 908–912. IEEE, 2001.

[51] Amin Khodaei. Microgrid optimal scheduling with multi-period islanding constraints. *Power Systems, IEEE Transactions on*, 29(3):1383–1392, 2014.

[52] Amin Khodaei, Shay Bahramirad, and Mohammad Shahidehpour. Microgrid planning under uncertainty. *IEEE Transactions on Power Systems*, 30(5):2417–2425, 2015.

[53] Johann W Kolar, Thomas Friedli, Florian Krismer, Andreas Looser, Mario Schweizer, Romeu A Friedemann, Peter K Steimer, and Joe B Bevirt. Conceptualization and multiobjective optimization of the electric system of an airborne wind turbine. *IEEE Journal of Emerging and Selected Topics in Power Electronics*, 1(2):73–103, 2013.

[54] Iordanis Koutsopoulos, Vassiliki Hatzi, and Leandros Tassiulas. Optimal energy storage control policies for the smart power grid. In *Smart Grid Communications, 2011 IEEE International Conf. on*, pages 475–480. IEEE, 2011.

[55] Ponnambalam Kumaraswamy. A generalized probability density function for double-bounded random processes. *Journal of Hydrology*, 46(1-2):79–88, 1980.

[56] M Kunz, B Mühr, T Kunz-Plapp, JE Daniell, B Khazai, F Wenzel, M Vannieuwenhuyse, T Comes, F Elmer, K Schröter, et al. Investigation of superstorm sandy 2012 in a multi-disciplinary approach. *Natural Hazards and Earth System Sciences*, 13(10):2579–2598, 2013.

[57] Elizaveta Kuznetsova, Carlos Ruiz, Yan-Fu Li, and Enrico Zio. Analysis of robust optimization for decentralized microgrid energy management under uncertainty. *International Journal of Electrical Power & Energy Systems*, 64:815–832, 2015.

[58] Robert Lasseter, Abbas Akhil, Chris Marnay, John Stephens, Jeff Dagle, Ross Guttromson, A Meliopoulous, Robert Yinger, and Joe Eto. The CERTS microgrid concept. *White paper for Transmission Reliability Program, Office of Power Technologies, US Department of Energy*, 2(3):30, 2002.

[59] Robert H Lasseter and Paolo Paigi. Microgrid: A conceptual solution. In *Power Electronics Specialists Conference, 2004. PESC 04. 2004 IEEE 35th Annual*, volume 6, pages 4285–4290. IEEE, 2004.

[60] Clare Leschin-Hoar. In alaska's remote towns, climate change is already leaving many hungry, Jul 2016.

[61] Miles Lubin, Daniel Bienstock, and Juan Pablo. Two-sided linear chance constraints and extensions. Text available at http://web.mit.edu/jvielma/www/publications/Two-sided-linear-chance.pdf, 2016.

[62] Miles Lubin, Yury Dvorkin, and Scott Backhaus. A robust approach to chance constrained optimal power flow with renewable generation. *IEEE Transactions on Power Systems*, 31(5):3840–3849, 2016.

[63] Chris Marnay, Raquel Blanco, Kristina S Hamachi, Cornelia P Kawaan, Julie G Osborn, and F Javier Rubio. Integrated assessment of dispersed energy resources deployment. *Lawrence Berkeley National Lab*, 2000.

[64] Chris Marnay, Joseph S Chard, Kristina S Hamachi, Timothy Lipman, Mithra M Moezzi, Boubekeur Ouaglal, and Afzal S Siddiqui. Modeling of customer adoption of distributed energy resources. *Lawrence Berkeley National Lab*, 2001.

[65] Salman Mashayekh, Michael Stadler, Gonçalo Cardoso, and Miguel Heleno. A mixed integer linear programming approach for optimal der portfolio, sizing, and placement in multi-energy microgrids. *Applied Energy*, 187:154–168, 2017.

[66] Salman Mashayekh, Michael Stadler, Goncalo Cardoso, Miguel Heleno, Sreenath Chalil Madathil, Harsha Nagarajan, Russell Bent, Marc Mueller-Stoffels, Xiaonan Lu, and Jianhui Wang. Security-constrained design of isolated multi-energy microgrids. Under review at IEEE transactions on Power Systems, 2017.

[67] Elahe Mashhour and SM Moghaddas-Tafreshi. Integration of distributed energy resources into low voltage grid: A market-based multiperiod optimization model. *Electric Power Systems Research*, 80(4):473–480, 2010.

[68] Shervin Mizani and Amirnaser Yazdani. Design and operation of a remote microgrid. In *Industrial Electronics, 2009. IECON'09. 35th Annual Conf. of IEEE*, pages 4299–4304. IEEE, 2009.

[69] Manish Mohanpurkar and Siddharth Suryanarayanan. Accommodating unscheduled flows in electric grids using the analytical ridge regression. *IEEE Transactions on Power Systems*, 28(3):3507–3508, 2013.

[70] Kip Morison, Prabha Kundur, and Lei Wang. Critical issues for successful on-line security assessment. *Real-Time Stability in Power Systems: Techniques for Early Detection of the Risk of Blackout*, page 147, 2005.

[71] Paul Myles, Joe Miller, Steven Knudsen, and Tom Grabowski. 430.01. 03 electric power system asset optimization. *Morgantown, WV: National Energy Technology Laboratory*, 2011.

[72] Harsha Nagarajan, Emre Yamangil, Russell Bent, Pascal Van Hentenryck, and Scott Backhaus. Optimal resilient transmission grid design. In *Power Systems Computation Conference (PSCC), 2016*, pages 1–7. IEEE, 2016.

[73] Apurva Narayan and Kumaraswamy Ponnambalam. Risk-averse stochastic programming approach for microgrid planning under uncertainty. *Renewable Energy*, 101:399–408, 2017.

[74] DB Nelson, MH Nehrir, and C Wang. Unit sizing and cost analysis of stand-alone hybrid wind/pv/fuel cell power generation systems. *Renewable energy*, 31(10):1641–1656, 2006.

[75] Nps 100c-24 brochure – north america.

[76] Rodrigo Palma-Behnke, Carlos Benavides, Fernando Lanas, Bernardo Severino, Lorenzo Reyes, Jacqueline Llanos, and Doris Sáez. A microgrid energy management system based on the rolling horizon strategy. *IEEE Transactions on Smart Grid*, 4(2):996–1006, 2013.

[77] Alessandra Parisio and Luigi Glielmo. A mixed integer linear formulation for microgrid economic scheduling. In *Smart Grid Communications, 2011 IEEE International Conf. on*, pages 505–510. IEEE, 2011.

[78] María Pérez-Ortiz, Silvia Jiménez-Fernández, Pedro A Gutiérrez, Enrique Alexandre, César Hervás-Martínez, and Sancho Salcedo-Sanz. A review of classification problems and algorithms in renewable energy applications. *Energies*, 9(8):607, 2016.

[79] Md Mustafizur Rahman, Md Mohib-Ul-Haque Khan, Mohammad Ahsan Ullah, Xiaolei Zhang, and Amit Kumar. A hybrid renewable energy system for a north american off-grid community. *Energy*, 97:151–160, 2016.

[80] Line Roald and Göran Andersson. Chance-constrained ac optimal power flow: Reformulations and efficient algorithms. *arXiv preprint arXiv:1706.03241*, 2017.

[81] F Javier Rubio, Afzal S Siddiqui, Chris Marnay, and Kristina S Hamachi. CERTS customer adoption model. *Lawrence Berkeley National Lab*, 2000.

[82] A Saif, K Gad Elrab, HH Zeineldin, S Kennedy, and JL Kirtley. Multi-objective capacity planning of a pv-wind-diesel-battery hybrid power system. In *Energy Conf. and Exhibition (EnergyCon), 2010 IEEE International*, pages 217–222. IEEE, 2010.

[83] Mario Sciulli. Remote off-grid microgrid design support tool research call. http://energy.gov/oe/articles/oe-announces-awardees-under-remote-grid-microgrid-design-support-tool-research-call, September 2015.

[84] Joohyun Shin, Jay H Lee, and Matthew J Realff. Operational planning and optimal sizing of microgrid considering multi-scale wind uncertainty. *Applied Energy*, 195:616–633, 2017.

[85] Afzal S Siddiqui and Chris Marnay. Distributed generation investment by a microgrid under uncertainty. *Energy*, 33(12):1729–1737, 2008.

[86] Afzal S Siddiqui, Chris Marnay, Jennifer L Edwards, Ryan Firestone, Srijay Ghosh, and Michael Stadler. Effects of carbon tax on microgrid combined heat and power adoption. *Journal of Energy Engineering*, 2005.

[87] Kristina Skierka and Christine Eibs Singer. "New deal for energy" a big deal for africa, off-grid, Jan 2016.

[88] Brian Stott, Ongun Alsac, and Alcir J Monticelli. Security analysis and optimization. *Proceedings of the IEEE*, 75(12):1623–1644, 1987.

[89] Kaarthik Sundar, Harsha Nagarajan, Miles Lubin, Line Roald, Sidhant Misra, Russell Bent, and Daniel Bienstock. Unit commitment with n-1 security and wind uncertainty. In *Proceedings of the 19th Power Systems Computation Conference*, 2016.

[90] Kaarthik Sundar, Harsha Nagarajan, Line Roald, Sidhant Misra, Russell Bent, and Daniel Bienstock. A modified benders decomposition for chance-constrained unit commitment with n-1 security and wind uncertainty. *arXiv preprint arXiv:1703.05206*, 2017.

[91] Dan T Ton and Merrill A Smith. The us department of energy's microgrid initiative. *The Electricity Journal*, 25(8):84–94, 2012.

[92] Eneko Unamuno and Jon Andoni Barrena. Hybrid ac/dc microgrids—part i: Review and classification of topologies. *Renewable and Sustainable Energy Reviews*, 52:1251–1259, 2015.

[93] Ran Wang, Ping Wang, Gaoxi Xiao, and Shimin Gong. Power demand and supply management in microgrids with uncertainties of renewable energies. *International Journal of Electrical Power & Energy Systems*, 63:260–269, 2014.

[94] Peter Wong. Electricity monthly update. `http://www.eia.gov/electricity/monthly/update/`, December 2015.

[95] Allen J Wood and Bruce F Wollenberg. *Power generation, operation, and control*. John Wiley & Sons, 2012.

[96] Hongyu Wu, Mohammad Shahidehpour, Zuyi Li, and Wei Tian. Chance-constrained day-ahead scheduling in stochastic power system operation. *IEEE Transactions on Power Systems*, 29(4):1583–1591, 2014.

[97] Emre Yamangil, Russell Bent, and Scott Backhaus. Resilient upgrade of electrical distribution grids. In *AAAI*, pages 1233–1240, 2015.

[98] Daniel Yergin. Congratulations, america. you're (almost) energy independent, November 2013.

[99] Miguel Zamarripa, Pablo A Marchetti, Ignacio E Grossmann, Tejinder Singh, Irene Lotero, Ajit Gopalakrishnan, Brian Besancon, and Jean André. Rolling horizon approach for production–distribution coordination of industrial gases supply chains. *Industrial & Engineering Chemistry Research*, 55(9):2646–2660, 2016.

[100] Y Zinchenko, H Song, and W Rosehart. Optimal transmission network topology for resilient power supply. In ILS Conference 2016, editor, *Proc. 6th International Conference on Information Systems, Logistics and Supply Chain*, page 9, Bordeaux, France, 6 2016. ILS Conference 2016. Bordeaux, France.